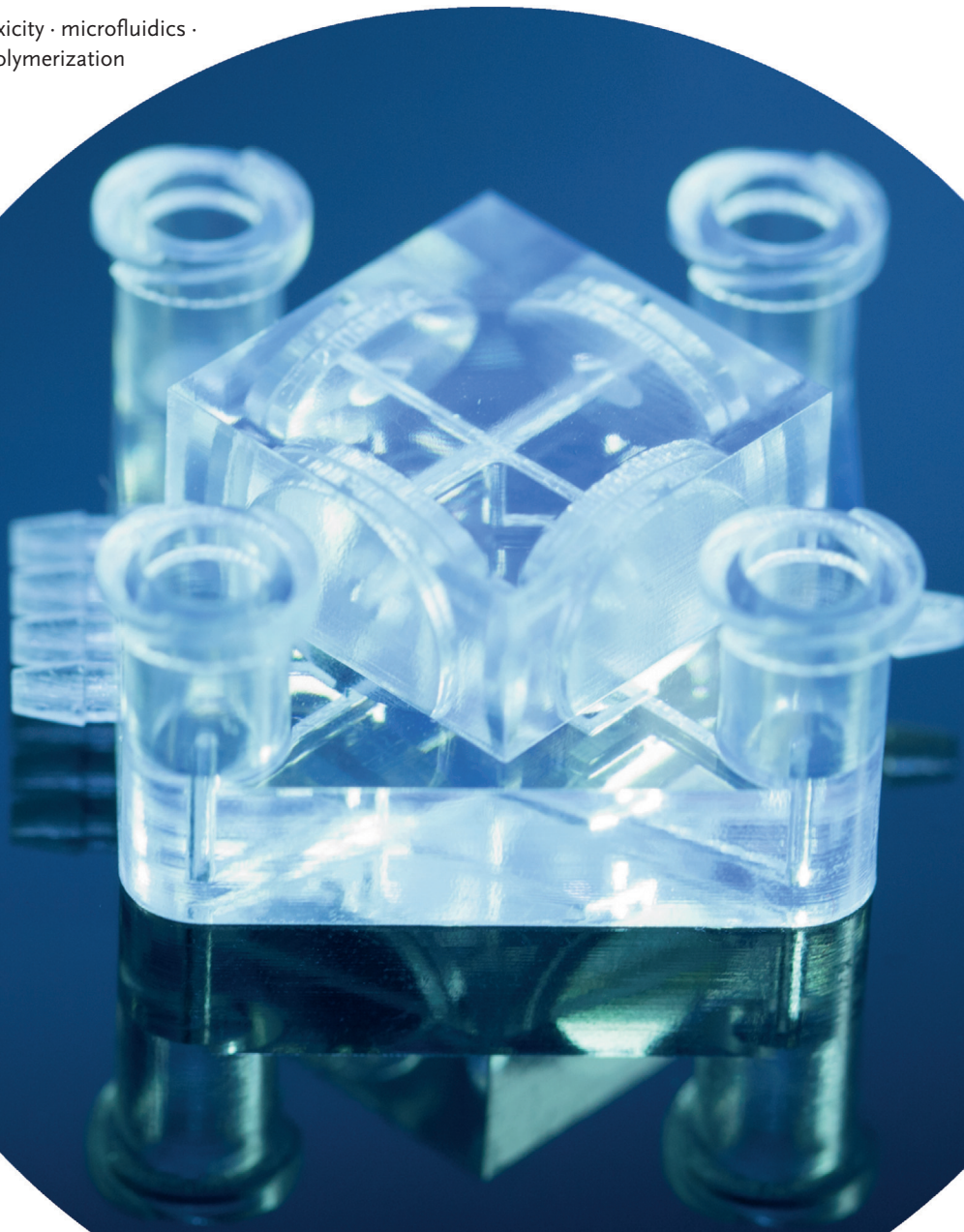


**3D Printing**International Edition: DOI: 10.1002/anie.201504382  
German Edition: DOI: 10.1002/ange.201504382

# 3D-Printed Microfluidics

*Anthony K. Au,\* Wilson Huynh, Lisa F. Horowitz, and Albert Folch***Keywords:**

3D printing · cytotoxicity · microfluidics · photochemistry · polymerization



The advent of soft lithography allowed for an unprecedented expansion in the field of microfluidics. However, the vast majority of PDMS microfluidic devices are still made with extensive manual labor, are tethered to bulky control systems, and have cumbersome user interfaces, which all render commercialization difficult. On the other hand, 3D printing has begun to embrace the range of sizes and materials that appeal to the developers of microfluidic devices. Prior to fabrication, a design is digitally built as a detailed 3D CAD file. The design can be assembled in modules by remotely collaborating teams, and its mechanical and fluidic behavior can be simulated using finite-element modeling. As structures are created by adding materials without the need for etching or dissolution, processing is environmentally friendly and economically efficient. We predict that in the next few years, 3D printing will replace most PDMS and plastic molding techniques in academia.

## 1. Introduction

Microfabricated devices, mostly in the form of microelectronic circuits and microelectromechanical (MEMS) sensors, have an increasing presence in myriad everyday objects—from smartphones, toys, and domestic appliances to laboratory, automotive, and wearable instruments. These devices owe their success to multiple factors: They are inherently fast, compact, mass-producible, and inexpensive, they consume small amounts of power, and some can even communicate with each other through wireless networks, which exponentially augments their individual computing capacity.

A newer type of microfabricated devices, microfluidic devices, can process miniature biomedical fluid samples down to picoliter and single-cell quantities. These devices have already revolutionized the fields of genome sequencing, proteomics, cell biology, and medical diagnostics by enabling inexpensive, customizable fluid-handling automation at the micrometer scale.<sup>[1]</sup> Microfluidic systems that integrate several functionalities, such as cell/tissue incubation controls, enzymatic processing, biochemical analysis, optoelectronic readouts, computer-controlled micropumps and microvalves, and/or wireless microcontroller capabilities, are generally termed “lab on a chip” or “MicroTAS” (also  $\mu$ TAS; TAS = total analysis system).<sup>[2]</sup> Owing to their low cost, small size, and multi-functionality—a critical combination of features not previously attainable—these integrated systems are expected to play a pivotal role in biomedicine, equivalent to the role that general microelectronic systems play in our daily life.<sup>[3]</sup>

The materials that are used for the generation of microfluidic systems have evolved to improve functionality. Early microfluidic systems were manufactured from glass and silicon. However, glass/silicon fabrication requires complex etching processes and is fundamentally limited to very planar, passive devices. The introduction of soft lithography<sup>[4]</sup>—a family of techniques based on molding the elastomer poly(dimethylsiloxane) (PDMS)—allowed for the production

## From the Contents

<b>1. Introduction</b>	3863
<b>2. 3D Printing Processes</b>	3864
<b>3. 3D-Printed Microfluidic Systems</b>	3869
<b>4. Salient Features of Stereolithography Compared to PDMS and Plastic Molding</b>	3872
<b>5. Summary and Outlook</b>	3878

of inexpensive polymeric devices and, for almost the same price, the integration of valves and pumps.<sup>[5]</sup> To date, the vast majority of microfluidic systems are still made from PDMS.<sup>[6]</sup> Indeed, PDMS is an inexpensive material that is easy to mold; its physicochemical properties are well suited for biomedical and physical sciences applications, and its design cycle lengths are generally adequate for prototype development.<sup>[6,7]</sup> For the fabrication of valves and pumps, PDMS is superior to plastics because the Young’s modulus of PDMS (ca. 2 MPa)<sup>[8]</sup> is approximately 1000 times smaller than that of hard plastics (hence PDMS valves and pumps can be built smaller and faster than their plastic counterparts).

However, the dissemination of PDMS-molded microfluidic systems among consumers faces several barriers. Figure 1 illustrates the three major technical barriers. First, most PDMS microfluidic systems incorporate cumbersome user

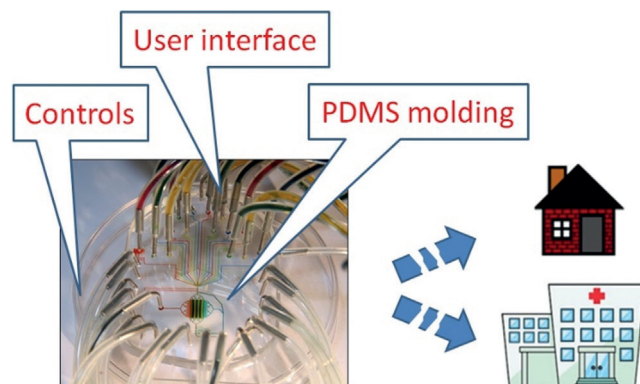


Figure 1. Major technical barriers for the dissemination of PDMS microfluidics to the consumer.

[\*] Dr. A. K. Au, W. Huynh, Dr. L. F. Horowitz, Dr. A. Folch  
Department of Bioengineering  
University of Washington  
3720 15th Ave NE, Box 355061, Seattle, WA 98195 (USA)  
E-mail: antau@uw.edu

interfaces based on hollow metal pins or other non-standard inlets that are prone to leaks. Microfluidic devices need to converge to industry-standard user interfaces—such as multi-well input systems—and leak-free connectors<sup>[9]</sup> that are intuitive to the user. Second, PDMS automation (valves, pumps)<sup>[5a,c]</sup> typically requires computer control and pneumatic switches that need highly skilled operators. To address this second challenge, microfluidic logic schemes containing “microfluidic transistors” and “microfluidic diodes” are being developed that allow the chips to run autonomously without external control systems.<sup>[10]</sup> The third barrier for dissemination is that PDMS molding is tediously slow. As society and funding agencies push for the translation of microfluidic systems into point-of-care applications, PDMS molding becomes an increasingly limiting strategy. The obvious alternatives—high-throughput molding techniques such as injection molding—are very expensive to implement and/or are not very adequate for incorporating valves and pumps. Financial barriers (e.g., the difficulty of gaining the interest of potential investors) can be considered surrogates of these barriers: If the technology did not have these dissemination barriers, investors would be more enthusiastic.

This Review explains how 3D printing has begun to help break these barriers. The number of publications with the keywords “microfluidics” and “3D printing” in Web of Science is, indeed, rising exponentially.<sup>[11]</sup> In contrast with soft lithography, 3D printing offers a commercialization-ready fabrication route for the integration of industry-standard user interfaces and embedded control systems in polymeric materials. For small production runs (from a single part to hundreds of parts), 3D printing is economical and allows for environmentally friendly efficiency (minimum waste and no tooling). Importantly, 3D printing benefits from all of the attributes of digital design: Remotely

interacting groups using CAD tools can design 3D-printed devices in modules, predict device performance with finite-element tools prior to printing, and precisely anticipate printing costs via a web interface<sup>[12]</sup>—a fabrication paradigm that is not routinely available for complex PDMS devices.

## 2. 3D Printing Processes

The term “3D printing”—considered to be synonymous with “solid freeform fabrication”—refers to a family of additive-based manufacturing techniques. Importantly, not all 3D printing techniques are suitable for microfluidics. The most widely used 3D printing techniques with relevance to microfluidics are selective laser sintering (SLS; Figure 2a), fused deposition modeling (FDM, also called “thermoplastic extrusion”; Figure 2b), photopolymer inkjet printing (Figure 2c), the similarly inkjet-based “binder jetting” (Figure 2d), laminated object manufacturing (LOM; Figure 2e), and stereolithography (SL; Figure 2f). As of today, the only 3D printing techniques that allow for the routine fabrication of closed microfluidic channels are SL and LOM, although the other techniques can also be applied to microfluidics by adding assembly steps. Efforts in bioprinting are also reviewed below because hydrogel printing might in the future be applied to the building of microfluidic systems.

### 2.1. Selective Laser Melting and Sintering

As in most 3D printing modalities, in selective laser melting/sintering (SLS), the object to be printed is digitally sliced into layers. The precursor “ink” material is a powder. A focused laser beam heats the powder material as it scans



**Anthony Au** obtained his B.S. in Biomedical Engineering at Johns Hopkins University in 2008 and his Ph.D. in Bioengineering at the University of Washington in 2014 under the direction of Prof. Albert Folch. He previously worked as an engineer at a biotech startup and as a research assistant at biotech companies and academic institutions. He is currently working on the development of wearable electronic devices.



**Lisa Horowitz** obtained her M.D. and Ph.D. in Neuroscience at Harvard Medical School under Prof. Linda Buck in 2000. She continued with postdoctoral studies on ion channel modulation with Bertil Hille at the University of Washington, before returning to work on olfaction with Linda Buck at the Fred Hutchinson Cancer Research Center. Since then, she has worked at the interface of microfluidics and biology, including projects on neuroscience, immunotherapy, and cancer treatment.



**Wilson Huynh** obtained his B.S. in Bioengineering at the University of Washington in 2014. As an undergraduate, he worked as a research assistant under the mentorship of Prof. Albert Folch. His research involved the development of user-friendly microfluidic devices for drug screening and personalized cancer therapies. He is currently working as a clinical assistant at a cancer research center in Seattle, Washington, where he is investigating the impacts of current cancer treatment modalities on patients.



**Albert Folch** obtained his Ph.D. in Nanotechnology from the University of Barcelona in 1994. He was a postdoc at MIT under Martin Schmidt and Mark Wrighton, and at Harvard under Mehmet Toner. He has been at the University of Washington since 2000 where he is an Associate Professor in Bioengineering. His research lies at the interface of microfluidics, neurobiology, and cancer. Since 2007, his lab has run an outreach art program called BAIT (Bringing Art Into Technology).

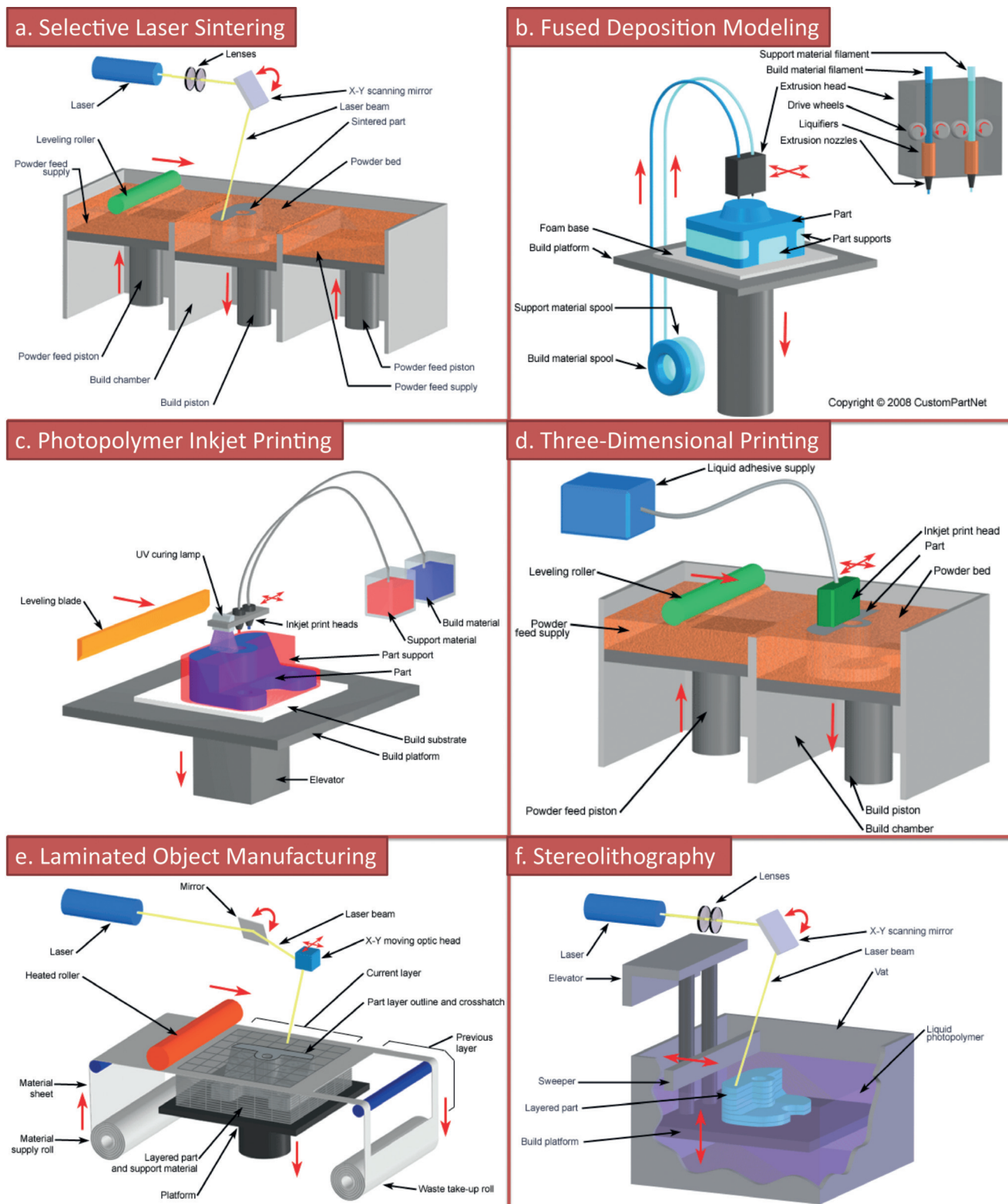


**Figure 2.** Various 3D printing techniques. a) Selective laser sintering (SLS). b) Fused deposition modeling (FDM, also termed “thermoplastic extrusion”). c) Photopolymer inkjet printing. d) Binder ketting, also trademarked as 3DP. e) Laminated object manufacturing (LOM). f) Stereolithography (SL). Images courtesy of CustomPartNet.com.

across the build area of the printer to define each layer of the object. After each layer has been exposed, the build plate is lowered further into the powder, and a roller dispenses

another thin layer of powder over the object (Figure 2b). At the end, the object must be retrieved from the bed where it is embedded in powder. This powder must be dusted off with

compressed air. When the precursor is a pure metal alloy, the technique is referred to as “selective laser melting” (SLM) and can be used to produce pure metal parts. When a variety of polymers are used in powder form, the laser fuses the powder by a thermal treatment (called “sintering”) rather than by fully melting the materials. This technique is referred to as “selective laser sintering” (SLS). Energy can also be delivered by means of an electron beam (“electron beam melting”, EBM).<sup>[13]</sup>

SLS has found numerous biomedical applications. Anatomically correct scaffolds for bone tissue repair or bone tissue engineering (e.g., customized maxillofacial or cranial implants) have been made from degradable and non-degradable biopolymers, ceramics, and composites; personalized devices for drug delivery or prosthetics and surgical models of specific organs based on medical imaging data (e.g., MRI or CT) have also been developed with SLS (see the Reviews in Ref. [14]). A polycaprolactone trachea implant was recently SLS-printed and successfully implanted into a newborn.<sup>[15]</sup> Biocompatible metals such as titanium are of paramount importance in the fabrication of implants, but they are also extremely expensive to manufacture owing to their hardness. SLS printing services (e.g., Renishaw)<sup>[16]</sup> now offer implant personalization (e.g., dental bridges and bone reconstruction).

Several factors explain the popularity of SLS. The advantage of this technique over other 3D printing techniques is that the powders produce materials that, when sintered, have a high purity and properties similar to those obtained by traditional fabrication processes. Furthermore, the machines can be designed to deliver various different powder precursors, which results in multi-material printing. SLS can also be used for writing metal patterns onto polymers such as PDMS,<sup>[17]</sup> a feature that could have applications in the design of biosensors. SLS is presently the rapid prototyping technique of choice for high-end, realistic industrial prototype design, as seen in the automotive and toy industry and for the development of sportswear and kitchenware, for example.

## 2.2. Photopolymer Inkjet Printing

Photopolymer inkjet printing is a simple, recently developed technique that has gained wide popularity in the consumer market. The concept of using inkjet printers to build 3D structures with curable polymers was first patented in 1999 (U.S. Patent 6259962) by Objet, an Israeli company that was acquired by Stratasys. Photopolymer inkjet printing is popularly also known as PolyJet or MultiJet Modeling (MJM; Figure 2c). Although the range of materials that can be printed with PolyJet technology is very large (soft and hard plastics as well as elastomers with many colors),<sup>[18]</sup> the material formulations are proprietary, so the user is forced to keep buying costly supplies, and bio- and cytocompatibility studies are lacking. PolyJet-printed anatomically correct models have been used to better plan medical procedures, such as orthopedic,<sup>[19]</sup> cardiac,<sup>[20]</sup> and intracranial aneurysm<sup>[21]</sup> surgeries. A similar technique called “binder jetting” (trademarked as “3DP”; Figure 2d), uses powder and a water-based

binding agent to produce 3D structures without resorting to expensive inks; 3D Systems sells multi-color 3DP machines. Both PolyJet and 3DP machines are capable of printing large objects (ca.  $20 \times 20 \times 20 \text{ cm}^3$ ) in multiple materials, even with working mechanisms (such as gears; the powder itself is used as a sacrificial material that is blown away at the end of the process) and metal circuits that can form field-effect transistors.<sup>[22]</sup> The final objects can be metallized or used as molds for metal casting.

## 2.3. Fused Deposition Modeling

Fused deposition modeling (FDM) consists of the extrusion of heated thermoplastic material from a positionable nozzle, hence the technique is also called “thermoplastic extrusion” (Figure 2e). The original FDM patent (U.S. Patent 5121329) was awarded in 1992 to Scott Crump, who founded Stratasys to commercialize the technology. FDM enables the printing of biocompatible and inexpensive polymers from spools of filament, such as acrylonitrile butadiene styrene (ABS, the polymer of Lego), poly(lactic acid) (PLA, a biodegradable polymer), polycarbonate, polyamide, and polystyrene. Since the expiration of the original patent, there has been a proliferation of FDM hardware companies (e.g., MakerBot), which have released increasingly inexpensive models, contributing to making 3D printing widely available and popular.

The structure of a material deposited in layers of filament differs from that of a bulk-reflowed solid (e.g., in injection molding). FDM-printed blocks are less dense and more prone to compressive stress fracture than their injection-molded counterparts because the filaments from adjacent layers are not well fused. These defects are mitigated (but not eliminated) in high-end machines in which the printed part is built within a heated enclosure.<sup>[23]</sup> FDM printing generates low levels of fumes during the exposure of plastics to high temperatures. These fumes pose a potential health hazard and would require additional ventilation equipment in future facilities containing many machines (for large-scale production).

In an alternative version of FDM, liquid precursors are extruded through a nozzle without heating. With this principle, FDM can be adapted to extrude a wide range of materials, such as metallic solutions, hydrogels, and cell-based solutions (see Section 2.6). Using this method, groups have created electronic components such as LEDs,<sup>[24]</sup> batteries,<sup>[25]</sup> strain sensors on flexible substrates,<sup>[26]</sup> antennas on 3D surfaces,<sup>[27]</sup> interconnects,<sup>[28]</sup> and electrodes within biological tissue,<sup>[29]</sup> for example. Therefore, the extrusion of liquid materials could be an inexpensive route to incorporate a variety of sensors and actuators within microfluidic devices, although the designers must develop practical solutions to the issues of assembly and bonding.

## 2.4. Laminated Object Manufacturing

In a low-cost technique called laminated object manufacturing (LOM), plastic, metal, and ceramic laminates are laser-cut and assembled layer-by-layer to fabricate devices. Glue or chemical bonding is used to stop the layers from detaching; aligning and stacking the layers during bonding can be done manually, with the aid of pins or by using specialized machines (Figure 2 f). When the cutting is performed with the tip of a physical plotter, the technique is referred to as “xurography”.<sup>[30]</sup> Most LOM work to date has focused on metal<sup>[31]</sup> or ceramic<sup>[31b]</sup> laminates, which are difficult to produce by other methods. Although LOM is technically not a fully additive manufacturing technique (it requires etching and the assembly of each layer), the manufacturing process can be fully specified from a digital file just like any other 3D printing process.

## 2.5. Stereolithography

In its original form, invented by Charles W. Hull in 1986 (U.S. Patent 4575330),<sup>[32]</sup> stereolithography (SL) consists of focusing a laser light source on a vat filled with liquid photopolymer resin; layer-by-layer selective polymerization produces 3D polymer structures<sup>[33]</sup> (Figure 2a). Hull originally described SL as a process using a “UV-curable material”, but modern high-intensity laser and focused LED light sources can achieve polymerization in the visible-wavelength range with suitable types of photoinitiator.<sup>[34]</sup> In

traditional SL, resolution (minimum achievable feature width) is determined mostly by the laser spot size and the resin type. As different resins have different light absorption spectra, they have different light penetration depths. Thus the same exposure parameters can result in completely different structures for different resins. Instead of sequentially scanning a laser over each feature in a layer of resin as in traditional SL, an alternative form of SL uses digital light projection (DLP) to crosslink an entire layer of resin at once. This strategy was first demonstrated with a liquid crystal display (LCD)<sup>[35]</sup> but is now achieved with an inexpensive, commercially available projector featuring a digital micromirror display (DMD).<sup>[33b]</sup> In this form of SL, the minimum X-Y feature size is determined by the size of the projected pixel, which may be significantly smaller than the laser spot sizes used in conventional SL. In both forms of SL, the resin remaining in the vat after exposure may be reused.

In SL, the object is digitally sliced into layers and printed by focusing the light source over the closest surface of the liquid. There are two strategies for resin exposure (depending on whether photopolymerization occurs at the top or the bottom surface of the vat), and two different light sources for printing (laser or DLP). In the laser-based SL machines developed by 3D Systems, the metal build stage is submerged further into the resin-containing vat after the formation of each layer. As photopolymerization occurs at the top surface of the resin at the air interface, this configuration is known as the free surface technique (Figure 3a). Conversely, in most other laser- and DLP-based stereolithography machines, the metal build plate is suspended upside-down, and the photo-

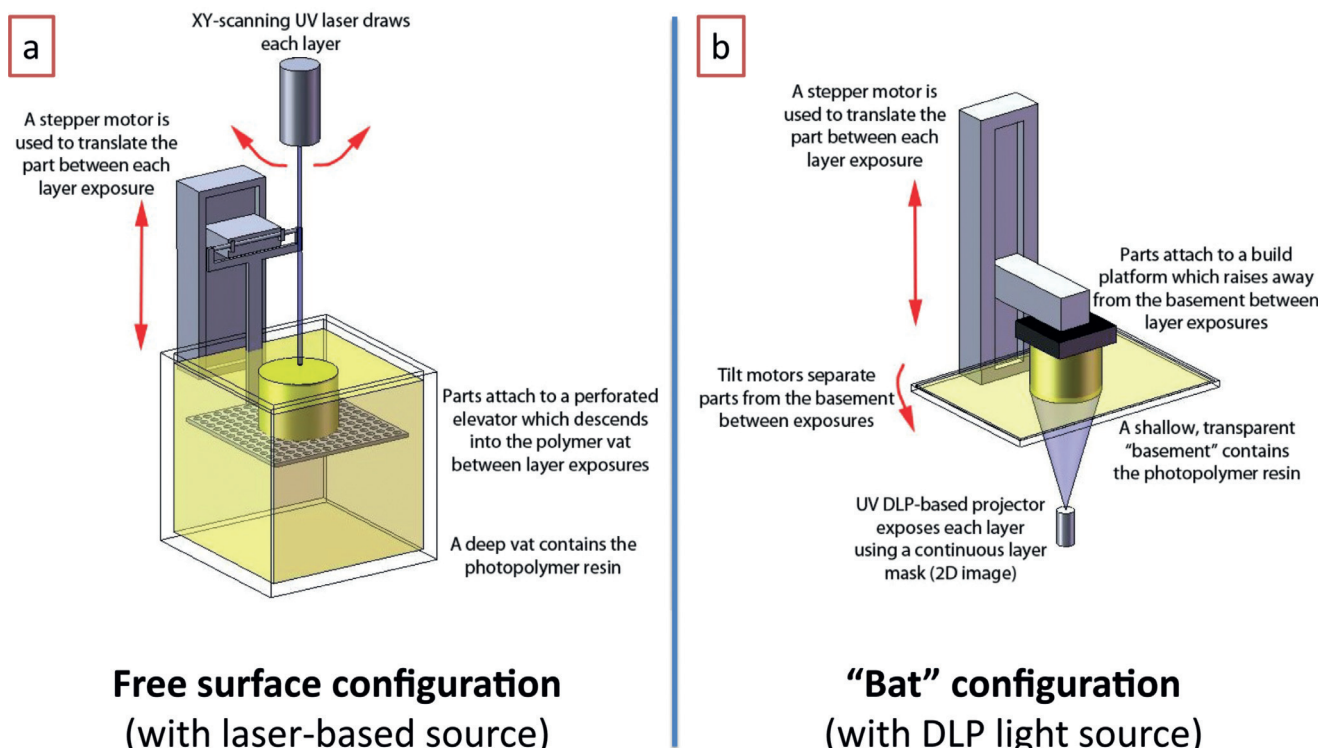


**Figure 3.** Two SL printing configurations. a) Laser-scanning SL with the free-surface configuration. b) DLP SL with the constrained-surface/“bat” configuration. Adapted from Ref. [39] with permission from IOP Publishing and David Dean.

polymerization occurs against the bottom surface of the resin vat. This configuration, known as the constrained surface technique (Figure 3b), is also referred to as the “bat” configuration<sup>[34]</sup> as the final part is oriented upside-down. The earlier free surface technique applies less mechanical force on the part being built when switching between layers, which may result in better structure fidelity. However, the “bat” configuration offers certain advantages,<sup>[36]</sup> namely 1) the part height is not limited by the vat depth; 2) the layer thickness that can be achieved is only determined by the Z stage resolution and independent of the viscosity of the resin; and 3) as curing happens away from the surface of the liquid resin, oxygen inhibition is minimized, and the resin can be cured faster. However, between each build layer, the printer must mechanically separate the most recently cured layer of the print from the bottom surface of the vat (usually coated with PDMS), a slow process that can deform fragile features. Recently, a modification of the bat configuration was introduced that exploits the controlled oxygen inhibition of the bottom-most layer of the resin. In this continuous-printing approach, the bottom plate is permeable to oxygen such that photopolymerized regions remain suspended in resin rather than adhering to the bottom substrate; by bypassing the layer separation step, the printing speeds were increased by a factor of 100.<sup>[37]</sup> Other continuous-printing approaches have been presented.<sup>[38]</sup>

Direct laser writing (DLW) is similar to but should not be confused with SL.<sup>[40]</sup> (To add to the confusion, the term “direct laser writing” has been used rather liberally in the literature.) DLW is based on the exposure of a photoresist layer by means of a laser that can be steered in three directions. As with SL, multiphoton optics may be used to achieve very high resolution. The fundamental difference between SL and DLW is that in SL, light exposure occurs within a liquid (the resin), whereas in DLW, light exposure occurs within the solid photoresist layer (after the solvent has evaporated). Hence, in DLW, development of the photoresist at the end of the exposure is required; therefore, DLW does not belong to the class of additive techniques—it is, like micromachining and photolithography, a “subtractive” technique in the sense that most of the base material (here, photoresist) is wasted. To fabricate microchannels with DLW, for example, the laser is used to change the solubility of the walls (or the core) in the developer, but selective dissolution of the microchannel core in the developer solution needs to follow. The high price of DLW systems (such as Nanoscribe)<sup>[41]</sup> renders their dissemination difficult. For simplicity, the small body of work on DLW-fabricated microfluidic channels is covered in the SL section.

## 2.6. Bioprinting

Bioprinting, also termed “organ printing”, has been defined as “the use of printing technology to deposit living cells, extracellular matrix (ECM) components, biochemical factors, proteins, drugs, and biomaterials on a receiving solid or gel substrate or liquid reservoir”.<sup>[42]</sup> Early implementations used direct laser writing approaches to deposit cells<sup>[43]</sup> or to

directly print cells with inkjet technology.<sup>[44]</sup> Extrusion pens (i.e., FDM using room-temperature liquids), electrospray, and selective photopolymerization have now been added to the arsenal of bioprinting technologies (see the Review in Ref. [45]).

Whereas these techniques have great potential for tissue engineering, their applicability to microfluidics is still on the horizon because in most cases, the transfer of the bio-ink onto a soft substrate makes it very difficult to predict the final 3D structure. It is noteworthy that SL systems have been successfully applied to bioprinting, for the long-term encapsulation of cells in hydrogels with high viability<sup>[46]</sup> (see the Review in Ref. [47]). SL allows the user to define heterogeneous scaffolds<sup>[48]</sup> of (cell-laden or not) extracellular matrix components and other long-term biocompatible hydrogels, including PEG diacrylate<sup>[48,49]</sup> (Figure 4 a–c), gelatin methacrylate<sup>[50]</sup> (Figure 4 d,e), hyaluronic acid,<sup>[51]</sup> and PEGylated/functionalized alginates.<sup>[52]</sup> In principle, it should be possible

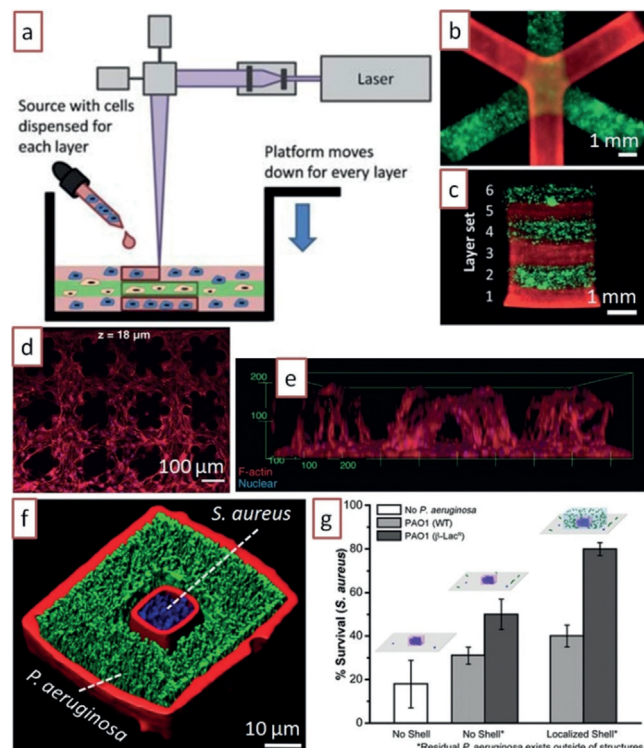


**Figure 4.** Bioprinting. a) Experimental setup for the patterned encapsulation of cells in PEG-based photo-crosslinkable hydrogels by means of SL. b) Top view of a multi-layer structure printed with the setup in (b), containing NIH 3T3 fibroblasts stained with CellTracker Green or Orange. c) Side view of the structure in (b). d) Confocal Z-optical section of a 3D cellular array of NIH 3T3 fibroblasts printed by SL in a gelatin-methacrylate scaffold. e) Side view of the structure in (d). f) Microclusters of the bacterium *S. aureus* printed within high-density populations of *P. aeruginosa* in BSA-gelatin microcontainers. g) The survival of *S. aureus* confined to the microclusters in (f) is significantly enhanced. Panels (a)–(c) reproduced from Ref. [49b] with permission from The Royal Society of Chemistry. Panels (d) and (e) reproduced from Ref. [50b] with permission from John Wiley and Sons. Panels (f) and (g) reproduced from Ref. [55], Copyright 2013 National Academy of Sciences, USA.

to define complex scaffolds that could serve as microfluidic vasculature mimics or even “living cellular machines”.<sup>[53]</sup>

In bioprinting, the choice of photosensitizer molecule that initiates the photo-crosslinking reaction is key because it affects cell viability. Shear et al. photo-crosslinked gelatin and other proteins using methylene blue or rose bengal as photosensitizers, thus bypassing the use of less biocompatible methacrylated polypeptides (e.g., Irgacure 2959)<sup>[54]</sup> as cross-linking agents. With a DMD-masked multiphoton system, they 3D-printed gelatin chambers that encapsulated closely interacting bacterial ecosystems<sup>[55]</sup> (Figure 4 f,g).

### 3. 3D-Printed Microfluidic Systems

#### 3.1. Fabrication by Stereolithography

In SL, microchannels are defined by polymerizing the walls of the channel cavities and subsequently draining the uncured photopolymer precursor. The minimum achievable microchannel cross-section is influenced by the viscosity of the photopolymer precursor, by the type of resin, and by the experience of the operator with channel draining.<sup>[12]</sup> Renaud and co-workers developed an SL setup based on a dynamic pattern generator (Figure 5a) with which they fabricated the first SL-printed microfluidic device, a mixer with a complex internal 3D architecture that could not be produced by molding (Figure 5b).<sup>[56]</sup> In this efficient mixer, fluids were fully mixed after a length of 4 mm at  $Re = 12$  (Figure 5c).

Multiphoton optics can be used to increase the resolution of the exposure. A microfluidic micromixer with approximately 10  $\mu\text{m}$  wide internal channels (wall width ca. 1  $\mu\text{m}$ ) was fabricated by DLW in the photoresist SU-8 (Figure 5d,e).<sup>[57]</sup> Shear and co-workers used digital micromirror devices (DMDs) and multiphoton optics to produce high-resolution 3D protein structures as stacks of 2D tomographic slices, which were serially printed with sub-micrometer resolution using methylene blue as the photosensitizer.<sup>[58]</sup> Some of the features contained fluidic cavities, such as a microchamber to direct bacterial motility<sup>[58,59]</sup> (Figure 5 f–h).

#### 3.2. Fabrication by Selective Laser Sintering

SLS lends itself to the fabrication of small metallic parts, such as interdigitated-electrode supercapacitors.<sup>[60]</sup> The aerospace and automotive sectors are now considering the production (not just prototyping) of small, intricate titanium parts by SLS owing to the lower fabrication cost by SLS compared to traditional manufacturing methods (in aerospace engineering, every 100 kg saves \$2.5 millions in fuel).<sup>[61]</sup> However, the solid (non-flowing) nature of the powder precursor renders microfluidic applications challenging. Titanium and stainless-steel flow devices were recently produced by SLS; the powder precursor could be evacuated from 300 mm long tubes with a diameter of 3 mm, but clogged longer tubes<sup>[62]</sup> (Figure 6).

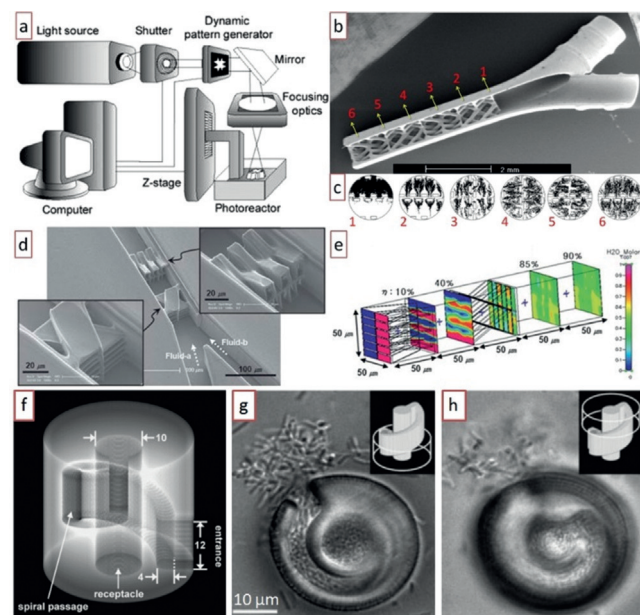


**Figure 5.** Microfluidic systems printed by stereolithography (SL). a) SL setup used to print the first microfluidic device. b) Scanning electron micrograph (SEM) of the first SL-printed microfluidic device, showing a microconnector. c) Numerical simulations of the device in (b) at the indicated locations. d) SEM of a micromixer printed in SU-8 by direct laser writing (DLW). e) Numerical simulation of the mixing performance of the device printed in (d); the mixing efficiency  $\eta$  measured at a distance five times the width of the channel is  $\eta = 90\%$  for  $Re = 1$ , and the Péclet number is 1000. f) Digital representation of a microfluidic “lobster trap” for bacteria; this structure was fabricated in bovine serum albumin in about 2 min from a sequence of 120 masks, each one separated by a 0.3  $\mu\text{m}$  vertical step of the focal plane. g) An *E. coli* colony forming at the bottom of the lobster trap. h) Overnight incubation of the colony resulted in growth of the colony into the upper portion of the trap. Panel (a) reproduced from Ref. [33b] with permission from the authors. Panels (b) and (c) reproduced from Ref. [56] with permission of The Royal Society of Chemistry. Panels (d) and (e) reproduced from Ref. [57] with permission from The Royal Society of Chemistry. Panels (f) to (h) reproduced from Ref. [58] with permission from John Wiley and Sons.

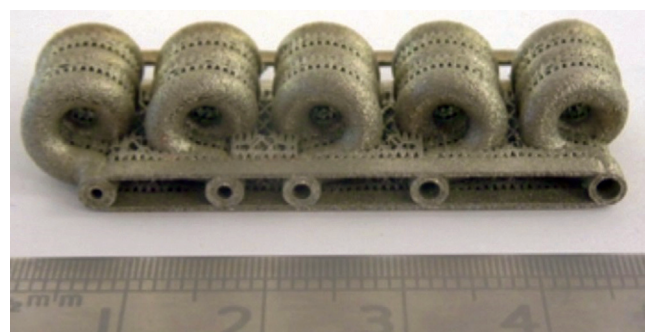


**Figure 6.** Stainless-steel flow device printed by selective laser sintering (SLS). Reproduced from Ref. [62] with permission from The Royal Society of Chemistry.

#### 3.3. Fabrication by Photopolymer Inkjet Printing

High resolution and the inherent multi-material printing capability makes photopolymer inkjet printing, or PolyJet,

a very promising technology. Straight microfluidic channels printed in VeroClear (a translucent acrylate-based material supplied by Stratasys) have been cleared mechanically by means of capillaries (scraping), sonication, and compressed air<sup>[63]</sup> (Figure 7a); channels of widths smaller than 500 µm

closed when a lid was assembled separately.<sup>[65]</sup> Another source of concern is that the printed resins have not been optimized or characterized for cytocompatibility, and they have a residual smell that suggests the presence of persistent, potentially non-cytocompatible compounds.

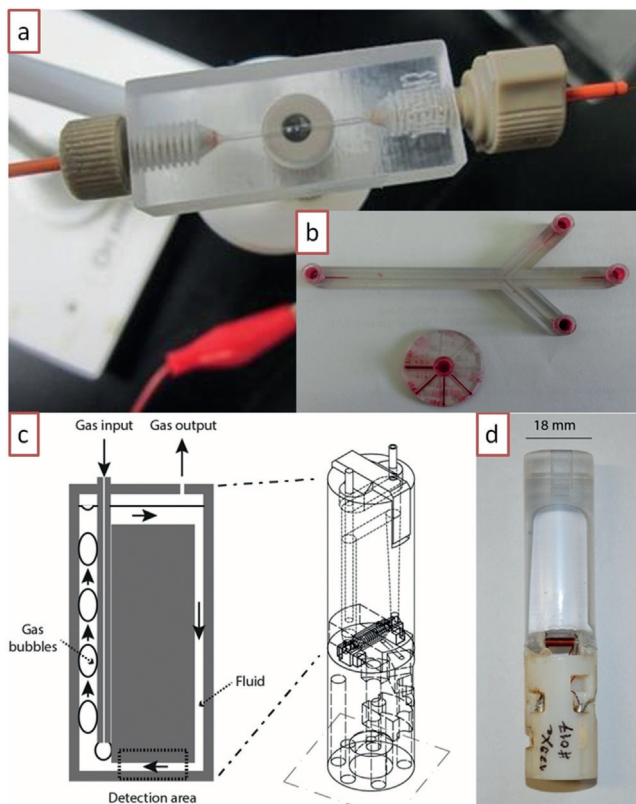


**Figure 7.** Microfluidic devices printed by PolyJet. a) The channel is 500 µm wide and was mechanically cleared with a cylindrical probe. b) PolyJet test prints of two microfluidic devices; the core of the channel was defined with a sacrificial material, and dissolution was attempted with NaOH. The introduction of a red dye into the inlet demonstrates that small/very long channels cannot be cleared of the sacrificial material. c) Schematic representation and d) photograph of a nuclear magnetic resonance (NMR) bubble pump printed by PolyJet. Panel (a) reproduced from Ref. [63] with permission from The Royal Society of Chemistry. Panel (b) contributed by Rob Ameloot and Clement Achille. Panels (c) and (d) reproduced from Ref. [65] with permission from The Royal Society of Chemistry.

could not be cleared reliably. Microfluidic channels of arbitrary geometries have not yet been built in a single step by PolyJet because Stratasys and/or ZCorp (owned by 3D Systems) have not developed a material that can be used as a printable sacrificial material to print the volume of the channels. Stratasys is now testing a supposedly soluble support, but successful removal of this second material (with NaOH) in microchannels is challenging, as the removal process is diffusion-limited (Figure 7b). A two-material lid that serves to pressurize or pull vacuum from the inlet(s) of a microfluidic device has been inkjet-printed.<sup>[64]</sup> A bubble pump that featured vertical channels was easily printed by PolyJet technology, although the fluidic circuit could only be

### 3.4. Fabrication by Fused Deposition Modeling

FDM is topologically ill-suited for producing microfluidic devices because the extrusion process lays down filaments that cannot be arbitrarily joined at channel intersections (leaks are likely) and that are large relative to the size of the microchannels (see Figure 8a–c).<sup>[66]</sup> Although a search for “fluid” in Thingiverse,<sup>[67]</sup> MakerBot’s free website for exchanging non-commercial 3D designs, yields more than 200 FDM-printable designs with large features and that claim

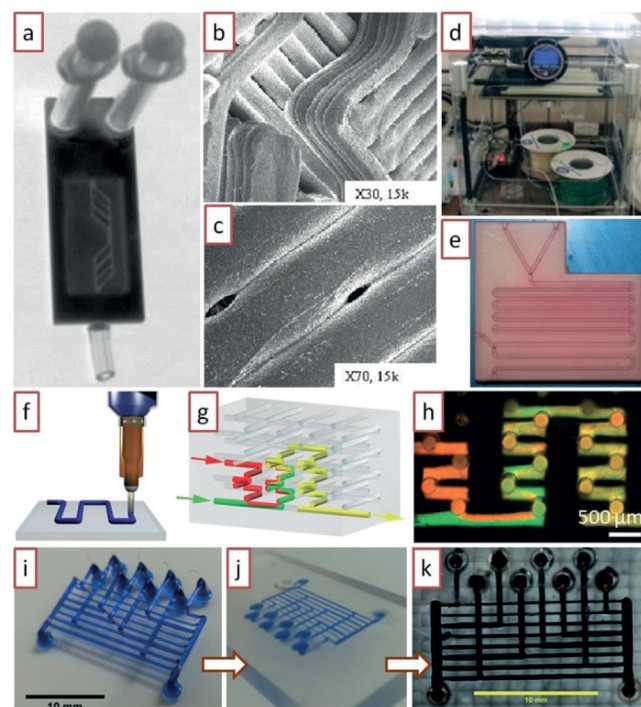


**Figure 8.** Microfluidic devices produced by molding features printed with fused deposition modeling (FDM). a) Optical micrograph of a microfluidic device printed by FDM. b,c) Scanning electron micrographs of the device in (a), showing that the walls are formed by joining plastic extruded structures (b) that are prone to form pores (c). d) The 3D printer 3DTouch. e) Microfluidic device printed in polypropylene by FDM with the 3DTouch printer. f) The principle of polymer extrusion. g) Schematic representation of a 3D microfluidic mixer after the sacrificial polymer has been removed. h) Optical micrograph of a complex 3D microfluidic mixer in operation. i) FDM-printed sacrificial isomalt scaffold. j) Embedding of the scaffold in (i) in agarose for casting; the carbohydrate quickly dissolves in the agarose hydrogel. k) Filling of the scaffold replica with black dye. Panels (a)–(c) reproduced from Ref. [66] with permission from the authors. Panels (d) and (e) reproduced from Ref. [72] with permission from The Royal Society of Chemistry. Panels (f)–(h) reprinted from Ref. [69] with permission from Macmillan Publishers Ltd: Nature Materials, copyright 2003. Panels (i)–(k) reproduced from Ref. [71] with permission from The Royal Society of Chemistry.

to hold fluid (such as a “fluidic vortex” or a “fluidic amplifier”), data are very sparse and qualitative. A flow device with a 3 mm diameter tube made by FDM in ABS polymer was recently reported;<sup>[62]</sup> however, the 5 mm thick walls of the device leaked in several places upon 20 bar pressurization. The ability of the 3D-printed filaments to seal with each other upon extrusion is probably a complex function of the material, the extrusion parameters, the equipment, the channel design, and the fluids used to fill the channel. Using a 3DTouch 3D printer (Figure 8d), Cronin and co-workers successfully printed 800  $\mu\text{m}$  wide polypropylene channels and demonstrated the flow of aqueous dye solutions (Figure 8e). In a variation of this setup, they used a custom-made printer to extrude acetoxy silicone polymer and built “reaction ware”,<sup>[68]</sup> which contained the fluids, although with no fluidic circuitry.

FDM has also been used to create channel volumes as a sacrificial material. After it has been surrounded by a different wall material, the channel material is removed. Lewis and co-workers fabricated complex microfluidic mixers with this approach: They printed complex 3D scaffolds of cylindrical segments using an organic ink (Figure 8f), infiltrated the scaffold with a UV-curable epoxy resin, and thermally extracted the organic ink by heating to 60°C<sup>[69]</sup> (Figure 8g,h). Similarly, a team led by Chen and Bhatia printed a 3D lattice of carbohydrates, which was subsequently infiltrated with ECM and living cells. The carbohydrate lattice could be dissolved with cell culture media, and the void space was seeded with endothelial cells to create vascular networks.<sup>[70]</sup> This approach inspired Bhargava<sup>[71]</sup> and co-workers to extrude sacrificial lattices made in isomalt, a sugar alcohol with a glass transition temperature of 55°C (Figure 8i). When cast in an agarose mold (Figure 8j), the sugar dissolved into the hydrogel in a matter of minutes, leaving a network that could be perfused with dye (Figure 8k). Whereas this technique is very intuitive, it is limited to circular-channel cross-sections (without in-channel features) and to a very special type of channel junctions (those formed by orthogonal cross-overs), which may not be suitable for certain key applications (e.g., cell separations or cell reactors).

### 3.5. Fabrication by Laminated Object Manufacturing

Before the advent of paper microfluidics,<sup>[73]</sup> LOM was an attractive option to rapidly prototype low-cost diagnostic devices, as shown by Yager and co-workers for a number of applications: Mylar lamination devices were produced to concentrate and separate proteins on the basis of isoelectric focusing,<sup>[74]</sup> to generate a rapid immunoassay,<sup>[75]</sup> to produce electrophoresis,<sup>[76]</sup> to lyse cells and extract proteins,<sup>[77]</sup> and to reconstitute functional proteins from an anhydrous storage depot,<sup>[78]</sup> among other applications. LOM has also enabled the prototyping of highly complex 3D microfluidic devices. Neils and Folch built a nine-layer Mylar laminate stack comprising six fluid layers, which functioned as a combinatorial mixer<sup>[79]</sup> (Figure 9a). A serpentine micromixer has also been built by xurography.<sup>[30]</sup> Rasooly and co-workers stacked five polycarbonate layers and one PMMA layer to produce a miniature

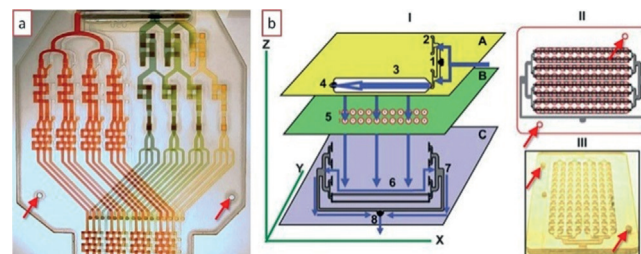


**Figure 9.** Microfluidic devices built by laminated object manufacturing (LOM). a) Combinatorial mixer built by LOM from nine Mylar laminates. b) A 96-well ELISA test built by LOM using one PMMA layer and five polycarbonate layers. For both devices, alignment between the different layers was ensured by fitting pre-patterned holes (arrows) in each layer through two vertical pins. Panels (a) and (b) reproduced from Refs. [79] and [80], respectively, with permission from The Royal Society of Chemistry.

96-well ELISA test (Figure 9b).<sup>[80]</sup> Despite clever improvements,<sup>[81]</sup> LOM is still limited by the channel network topologies that can be produced and by the debris accumulated during laser cutting and/or gluing, which can partially clog the channels or contaminate the samples. A European consortium has developed a competing photolithography-based process, named LABONFOIL, to laminate multilayer microfluidic devices in negative photoresist (polyimide or SU-8),<sup>[82]</sup> however at a considerable cost of €2 cm<sup>-2</sup>.

### 3.6. Comparison of Techniques

The various 3D printing techniques have different degrees of resolution and automation, as shown in Figure 10. In this graph, the traditional high-resolution patterning methods (DLW, photolithography, soft lithography) appear in the top left corner because they require large amounts of manual labor (with soft lithography being the most “manual”). 3D printing techniques, on the other hand, appear clustered in the bottom right corner because they typically feature less resolution and are highly automated, although they are not all equally automated. On one end of the spectrum, PolyJet

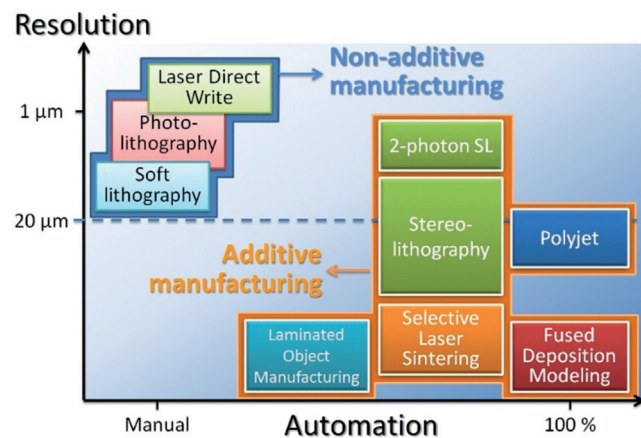


**Figure 10.** Resolution and automation trade-off in the transition from non-additive to additive manufacturing.

and FDM do not require any input from the user, and on the other end of the spectrum, LOM requires substantial assembly; somewhat in the middle, SL and SLS require some post-processing (cleaning the resin or powder). In terms of resolution, only SL and PolyJet have been able to cross the “magical line” of 20 µm (the size of some cells) where bio-microfluidic structures start to become particularly interesting. For a detailed comparison of a wider range of prototyping techniques applied to the fabrication of microfluidic devices, see Ref. [34].

#### 4. Salient Features of Stereolithography Compared to PDMS and Plastic Molding

Traditionally, SL has been perceived by many micro-fabrication researchers as being inferior to soft lithography in various key aspects (Figure 11), but opinion is quickly changing. Soft lithography benefits from the high resolution of the molds produced by photolithography and the high biocompatibility of PDMS, but suffers from low throughputs

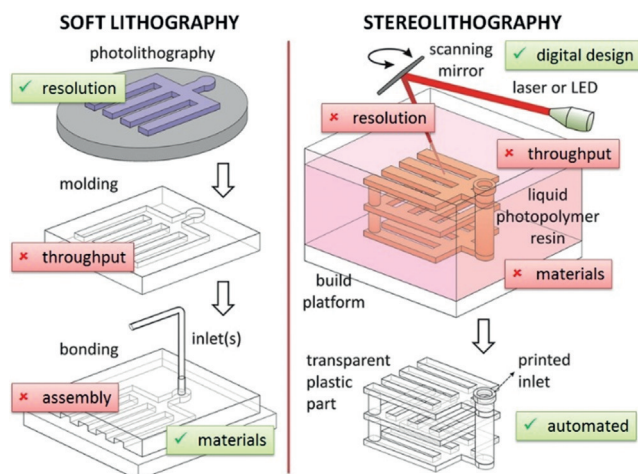


**Figure 11.** A conceptual overview of the advantages and disadvantages of soft lithography and stereolithography as traditionally perceived by researchers.

and unreliable assembly and bonding processes, resulting in layered designs and poor user friendliness. SL has a set of features that are almost opposite to those of PDMS: SL benefits from the full-digital design of 3D architectures and automated fabrication (which enables fabrication by service providers), but the resolution of standard SL machines is inferior to that of PDMS molding, and most SL resins are not biocompatible. Previously, we estimated that the cost of ordering a single SL-printed device from a service provider is roughly equivalent to the cost of fabricating an SU-8 master mold.<sup>[12]</sup> On a commercial SL machine, devices covering a build area of 125 × 125 mm<sup>2</sup> or larger may be printed in under ten hours.

#### 4.1. 3D Capability

PDMS and molded plastic microfluidic devices must be built by stacking layers, and the layers must be bonded together (e.g., see Ref. [83]). This process severely restricts the structures, connectivity, and functionality of the devices that can be built. SL is essentially an assembly-free digital manufacturing technique, so manufacturing complexity and manufacturing variety come at no cost. The functionality or connectivity of a given part has only dimensional restrictions (the part has to be built larger than the machine’s resolution) but has few topological restrictions, which creates opportunities for design innovation. (Note that when printing with a single material, the need for digital slicing and printing in the presence of gravity prohibits the printing of “floating objects”—for example, an unsupported sphere must be tethered.) In some embodiments of SL, it is possible to build parts in more than one material<sup>[84]</sup> (i.e., two-material parts that have varying material properties; see Section 4.4), which offers an even richer spectrum of design possibilities.

#### 4.2. Resolution and Throughput

At present, the “3D freedom” afforded by single-photon SL comes at the cost of lower resolution compared to PDMS/plastic-based devices. The high cost of two-photon laser setups still impedes their wide dissemination in the consumer market, so multiphoton systems remain largely academic.<sup>[57,58]</sup> All SL desktop systems use single-photon optics (laser or LED source). A quick survey of the available SL services shows that they can build (closed) microchannels that typically measure 500 × 500 µm<sup>2</sup> or larger in cross-section, although the machines can fabricate smaller open-surface features (e.g., open trenches). In other words, the limitation is not due to optics. Thus the main (legitimate) concern of microfluidic users is that the resolution of SL is lower than the resolution they are used to working with. Like soft lithography, SL is perceived as suffering from poor throughputs. However, recent developments in SL technology demonstrate critical improvements in printing speed and resolution. The year 2014, with the expiration of key SL patents, saw the appearance of many companies rushing to innovate; in the span of a few months at the beginning of 2015, Ilios announced a printer with 25 µm XY resolution (6 µm Z layers) and capable of four-material prints,<sup>[85]</sup> Old World Labs announced another printer with <1 µm XYZ resolution,<sup>[86]</sup> and Carbon3D announced a printer capable of printing in minutes instead of hours (ca. 100 times faster) with 1 µm XYZ resolution.<sup>[37]</sup> Clearly, industry is now leading the innovation in resolution and throughput. Systems with <5 µm resolution for <\$10000 in less than one year are not far-fetched. However, the biocompatibility of the resins is still a concern and will be discussed in Section 4.4.1.

#### 4.3. Microchannel Drainage: Limitations in Resolution and Automated Fabrication

Even though laser light scattering and polymer precursor diffusion both impose fundamental limits on the resolution in SL, in practice, the resolution of closed channels depends on the drainage of the liquid polymer precursor that is trapped inside after a device has finished printing. For long channels, this “hydrodynamic limitation” can be more important than the limitation imposed by the photoreaction. Unfortunately, this subtlety is not well appreciated by most printing services. To improve resolution and to facilitate the drainage of otherwise dead-end features, an efficient strategy can be to incorporate drain structures (e.g., shortcut holes, channels, and/or temporarily “breakable” connectors) that reduce the hydrodynamic resistance of the resin’s exit path. An example of shortcut holes is shown in Figure 12. The newer generation of less viscous photopolymer resins will also facilitate drainage.

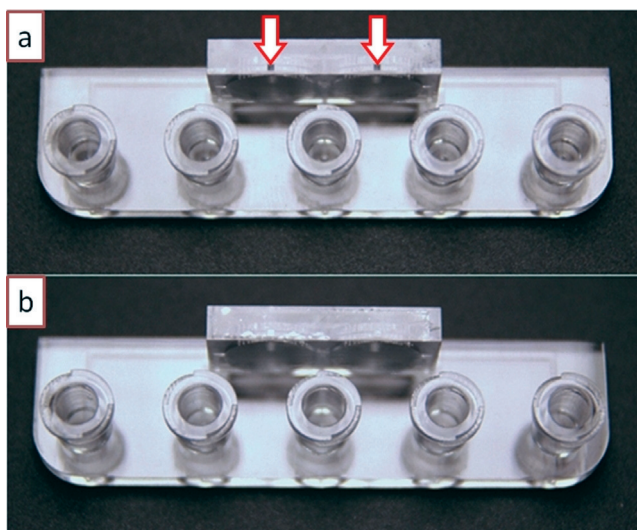


**Figure 12.** Implementation of drainage holes to simplify device architecture. a) In this device, the channels are fabricated with a square  $635 \times 635 \mu\text{m}^2$  outlet hole (indicated by arrows) so that the resin can be easily drained to the exterior. b) The drainage holes can be sealed with adhesive tape or epoxy. Reproduced from Ref. [87] with permission from The Royal Society of Chemistry.

The need for microchannel drainage at the end of the fabrication process leads to another important implication as it is a manual process that requires some preparations and it only permits automation for a given inlet layout. Therefore, 1) strictly speaking, SL, when applied to microfluidics, should be described as a quasi-automated, quasi-additive fabrication process (some post-processing and resin removal is necessary), 2) drainage results in additional setup time and post-fabrication handling that cannot be overlooked, especially for high-volume applications, and 3) drainage requires the use of (small amounts of) solvents, which adds to the disposal costs, and some equipment for powering the fluids, which incurs further capital cost.

#### 4.4. Material Considerations

Understandably, most microfluidic researchers, including our group, had fallen under the “spell” of PDMS for many years owing to the optimal properties of PDMS: PDMS is inexpensive, optically clear, elastomeric, biocompatible, and can be molded using simple methods. SL resins, on the other hand, have historically been costly, yellowish at best, and of questionable biocompatibility that has rarely been studied. Not surprisingly, most biomedical researchers have been reluctant to use them. However, the last few years have seen a great deal of innovation in this area.

##### 4.4.1. Biocompatibility

A number of biocompatible resins are now available. One of the most notable ones is a UV resin produced by DSM (Heerlen, Netherlands) under the trade name Somos WaterShed XC 11122. After printing, the cured WaterShed is rinsed with isopropyl alcohol and flood-exposed to UV light. At the end of this process, WaterShed is nearly colorless with a clarity, flexibility, and hardness similar to that of polycarbonate or poly(methyl methacrylate). (Prolonged exposure of WaterShed to UV gives it a yellowish tint.) Furthermore, it does not swell in water and meets biocompatibility standards ISO 10993-5 (cytotoxicity), ISO 10993-10 (sensitization), ISO 10993-10 (irritation), and USP Class VI. We have studied the cytocompatibility of C2C12 myoblast cell cultures on Matrigel-coated WaterShed for 24 hours and found no noticeable difference when compared to cells cultured on a Matrigel-coated polystyrene tissue culture (Figure 13a,b). Longer-term cytocompatibility on WaterShed awaits further investigation.

Additional biocompatibility data can be found in the drug delivery field, which has investigated the use of SL for the fabrication of implantable microneedles for more than one decade. Matsuda and Mizutani produced microneedles with a custom acrylate resin containing polycaprolactone;<sup>[90]</sup> loading of the microneedles with the anti-inflammatory drug indomethacin suppressed the foreign-body inflammatory reaction caused by the needles. Narayan and co-workers used e-Shell 200 and 300, commercially available acrylate-based polymers, to fabricate microneedles by SL<sup>[88]</sup> and DLW<sup>[91]</sup> (Figure 13c); these materials, which have been used to manufacture hearing aids, are water-resistant and Class IIa biocompatible. The same group has developed very sharp ceramic-like tips made from Ormocer<sup>[89,92]</sup> (Figure 13d,e), a material that has been used to produce high-resolution structures including 50  $\mu\text{m}$  wide channels.<sup>[93]</sup> These microneedles penetrated cadaveric porcine adipose tissue without fracture, and Ormocer surfaces supported the culture of human epidermal keratinocytes for three days without significant reduction in viability compared to control surfaces.

With some SL systems, photo-crosslinkable hydrogels and cells were successfully combined. PEG diacrylate,<sup>[48,49]</sup> gelatin methacrylate,<sup>[50]</sup> hyaluronic acid,<sup>[51]</sup> and PEGylated/functionalized alginates,<sup>[52]</sup> which are all highly biocompatible matrices, have been used to print cells encapsulated in hydrogel (see Figure 4), which were derivatized with adhesive ECM

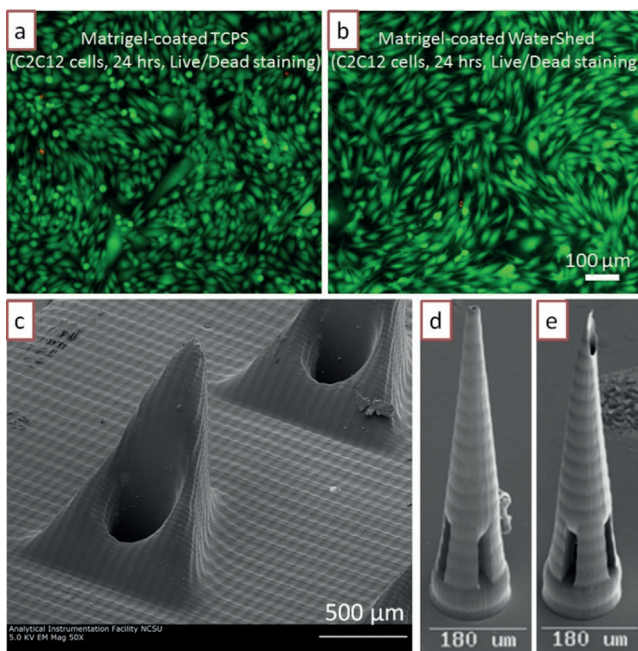


**Figure 13.** Biocompatibility of SL prints. a) C2C12 cells cultured on tissue culture polystyrene (TCPS) control surfaces coated with Matrigel; the cells were stained for viability with Live/Dead cell stain after one day in culture. b) C2C12 cells cultured on WaterShed surfaces coated with Matrigel using the same seeding and coating procedures as in (a); cell viability on WaterShed surfaces is indistinguishable from that on TCPS surfaces. c) SEM of hollow microneedles fabricated in e-shell 200 by DLP SL. d, e) SEM of microneedles fabricated in Ormocer by DLW. Panels (a) and (b) reproduced from Ref. [87] with permission from The Royal Society of Chemistry. Panel (c) reprinted from Ref. [88] with permission. Copyright 2011, AIP Publishing LLC. Panels (d) and (e) reproduced from Ref. [89] with permission from John Wiley and Sons.

proteins or cell-attachment peptide sequences. The cells used in these studies include fibroblasts,<sup>[49a]</sup> neurons, muscle cells,<sup>[52]</sup> and human mesenchymal stem cells.<sup>[94]</sup> These hydrogels have been envisioned to constitute parts of bio-actuators and biosensors that incorporate live cells.<sup>[53]</sup> Stampfl et al.<sup>[93]</sup> screened a number of acrylate-based monomers, combined them with diluents (water or PEG 400MW) and the photoinitiator Irgacure 819 to produce various hydrogel resins with a range of mechanical properties (with a Young's Modulus from 0.4 to 8000 MPa), and compared them to the commercially available resins Ormocer and Renshape. As soon as SL materials research moves to optimize materials for biomedical applications, we should see the birth of a new variety of SL resins that are biocompatible (even implantable and/or bioresorbable), transparent, and gas-permeable.

#### 4.4.2. PEG-DA, the Ideal Candidate

The field of cell encapsulation provides us with a great example of a photopolymerizable, biocompatible material: PEG diacrylate (PEG-DA), which has been extensively used as a hydrogel to trap cells and create 3D tissue constructs.<sup>[48,49,95]</sup> Photopolymerization processes require a photo-

initiator, a chemical compound that decomposes into free radicals or cations when exposed to light. Photoinitiators differ in their cytotoxicity, solubility in water, and stability. Intense efforts have been spent in developing and evaluating cytocompatible photoinitiators.<sup>[96]</sup> The photoinitiator Irgacure 2959 (Ciba) is frequently used with 325 nm light and can be utilized to encapsulate delicate cells, such as stem cells, with high viability.<sup>[97]</sup> The main challenge has been to find a biocompatible photoinitiator that works for light sources of the new generation of “desktop” SL systems ( $\lambda = 405$  nm, “near-UV”/visible light, which is more benign to cells). For 405 nm light, Irgacure 784 is available, but this compound is water-insoluble (must be dissolved in DMSO). Alternatively, lithium phenyl-2,4,6-trimethylbenzoylphosphinate (LAP, only recently commercially available) is water-soluble and very cytocompatible.<sup>[98]</sup> LAP has recently been re-discovered by Anseth and co-workers as a water-soluble type I photoinitiator that is uniquely active in the visible range ( $\lambda = 405$  nm and above).<sup>[98,99]</sup> This initiator has been shown to be cytocompatible, and has proved suitable for cell-encapsulation studies with PEG-DA.<sup>[98,100]</sup> It is important to stress that although the issue of the cytocompatibility of the photoinitiator should not be as relevant to building microfluidic devices as it is for encapsulating cells, it is desirable that photoinitiator molecules potentially leaching from the device walls be as cytocompatible as possible.

There is abundant evidence that PEG-DA is a very suitable material for microfluidics. Khademhosseini and Suh fabricated PEG-DA microchannels (by photolithography) and demonstrated that when using low-molecular-weight, heavily-crosslinked PEG-DA ( $M_w = 258$ ), the channels resisted swelling (and were impermeable to water) for up to two weeks, whereas higher-molecular-weight PEG-DA ( $M_w = 875$ ) showed significant swelling and collapse of the channels within five hours.<sup>[101]</sup> Woolley and co-workers produced PEG-DA microfluidic valves (by molding and layering)<sup>[102]</sup> and made an exhaustive evaluation of the various favorable properties of PEG-DA compared to glass, PDMS, and other polymers.<sup>[103]</sup> Thus PEG-DA seems to be an ideal resin for 3D-printable biomedical devices.

#### 4.4.3. Solvent Compatibility

PDMS is a very porous matrix that swells in organic solvents, which results in the loss of solvent into the micro-channel walls, detachment of the seal between the channels and the surface, and alterations of the channel geometries.<sup>[6]</sup> Therefore, many microfluidics research efforts have been directed towards developing polymer matrices that do not swell, especially microvalves, whose flexural element is made of Viton<sup>[104]</sup> or Teflon<sup>[105]</sup> in a chemically resistant micro-channel seat.

Research into SL resins has produced a variety of resins with a wide range of properties. Somos 9920, for example, is a durable resin whose properties mimic polypropylene, offering great chemical resistance. (Polypropylene is used to store solvents.) Somos 5530HT is also rated as solvent-resistant, water-resistant, and highly temperature-resistant. Somos 11120 (also termed “WaterShed”) is highly resistant to

water (but not organic solvents), transparent, and mechanically very strong.

#### 4.4.4. Wettability

Modulation of the wetting properties of SL resins is of paramount importance in microfluidics, as bubbles can form during filling and can be difficult to dislodge. SL-printed plastics do not have the high gas solubility of PDMS (which obeys Henry's law; i.e., the equilibrium concentration of a gas dissolved in PDMS is proportional to the partial pressure of gas present in the PDMS channels),<sup>[106]</sup> so the convenient method for dislodging bubbles from PDMS devices by pressurization of the fluids (which causes the bubbles to disappear into the PDMS walls) does not work in SL-printed plastic devices. Yang and co-workers added a vinyl-terminated initiator into the resin base (containing acrylate-based pre-polymers) to produce poly(ethylene glycol) methacrylate (PEGMA), a very hydrophilic and biocompatible polymer (which facilitated spontaneous filling, contact angle ca. 40°), or perfluorodecyl methacrylate (PFMA), a very hydrophobic polymer (contact angle ca. 123°;<sup>[107]</sup> Figure 14a,b). Hydrophobic coatings can be used to create aqueous partitions inside these devices.

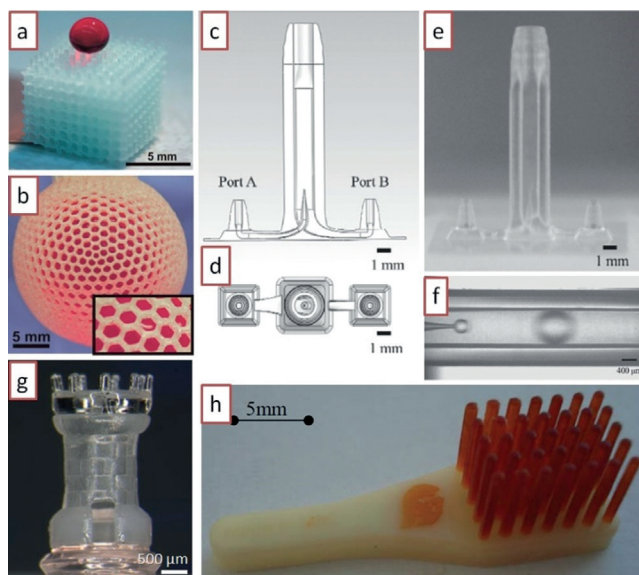


**Figure 14.** Multi-material SL printing. a) SL-printed cube in a super-hydrophobic resin; note that a droplet of dye deposited on the cube does not penetrate the cube. b) SL-printed sphere in a super-hydrophobic resin; the sphere is filled with dye, yet it does not leak through its 1 mm large hexagonal holes (see inset). c, d) Schematic side and top view, respectively, of a droplet generator. e) SL print of the device in (c); the inner channel has an internal diameter of 50 µm, and the fabrication accuracy is about 5 µm. f) Droplet generation in the SL-printed device shown in (e). (g) A three-material SL print; the chess piece has internal structure. h) A two-material SL print; the red tips are printed in an elastomeric resin. Panels (a) and (b) reproduced from Ref. [107] with permission from The Royal Society of Chemistry. Panels (c)–(f) reproduced from Ref. [110] with permission from the Japan Oil Chemists' Society. Panel (g) reproduced from Ref. [84a] with permission from Springer Science and Business Media. Panel (h) reproduced from Ref. [84b] with permission from the authors.

#### 4.4.5. Surface Derivatization and Bonding

Surface derivatization of printed SL resins has been achieved with commercially available silanes.<sup>[108]</sup> 3-Glycidoxypropyltrimethoxysilane (GPTMS) was used to create a siloxane layer on the surface of an epoxy-based resin under acidic conditions in the presence of a photoacid generator, triarylsulfonium hexafluoroantimonate (TASHFA), and UV light exposure. This chemistry was used to bond slabs of PDMS to the SL-printed resin. Epoxy slides have been used to chemically immobilize protein surface gradients by amine–epoxy linkage for chemotaxis experiments,<sup>[109]</sup> so in principle epoxy-based SL resins could be utilized to print chemotaxis devices. Another option is to derivatize the walls of the channel with a silicate coating, which produces a surface that is amenable to standard silane chemistry. Ohtani et al.<sup>[110]</sup> injected a hydrolyzed ethyl silicate solution (N-103X, Colcoat Co.) into the channel (part of a droplet generator,<sup>[111]</sup> see Figure 14c–e), then heated the device to 120°C for 30 min to vaporize the solvent and cure the coating on the walls. After the hydrophilic treatment, the silicate surface was derivatized with a fluorosilane compound to render it hydrophobic, which enabled the treated device to produce monodisperse inverted water-in-oil emulsions (Figure 14 f). Silane derivatization could enable silicate-like coatings made of allylhydridopolycarbosilane that confer polymer surfaces an electrophoretic mobility and a solvent resistance that (while retaining transparency) is indistinguishable from that of glass over at least 90 days.<sup>[112]</sup> We have found that WaterShed XC 11122 resin binds to O<sub>2</sub> plasma activated surfaces such as glass, polystyrene, or PDMS, provided the surfaces are heated above the glass transition temperature of the resin (ca. 42.5 °C).<sup>[113]</sup> This simple procedure circumvents the TASHFA and UV illumination steps described above.

#### 4.4.6. Multi-Material Stereolithography Printing

Although SL is traditionally regarded as a technique limited to printing in a single polymer material, recent advances in resins and SL printers have pushed the frontiers into multiple-material printing<sup>[84]</sup> (Figure 14g), including elastomers<sup>[84b]</sup> (Figure 14h) and ceramics.<sup>[114]</sup> Cho and co-workers observed that when they added copper microparticles to a photoresin, a sintering process rendered the microstructures conductive (resistivity ca. 10 times that of pure copper) with a shrinkage of 22–28%.<sup>[115]</sup> We can now foresee sensors and actuators containing parts that are flexible and/or metallic.<sup>[116]</sup> A new generation of multi-material printers<sup>[85]</sup> could allow for the creation of polymer gradients with new, interesting properties and for the printing of multi-material sensors and actuators.

#### 4.5. Digital Inspection and Finite-Element Modeling

One of the biggest advantages of SL (and 3D printing in general) is the ability to fully predict the performance of a device prior to printing it. The design can be sent via email and digitally inspected by a team of experts that is in a remote

location with respect to the design team. The inspection report can be easily returned and include amendments to the CAD design file. Inspection need not be limited to visualizing and correcting the architecture of the device. A researcher can now use finite-element modeling software to virtually test the expected mechanical performance, such as the flexural bending or the resonance frequency of a critical component, use fluid dynamics simulation software to test the performance of a mixer design, or both (in the case of a microvalve). Once the design “works” in the simulator, it can be printed. We predict that in the near future, this rational CAD approach to microfluidics will save an enormous amount of time and resources for complex projects.

#### 4.6. Overcoming the Barriers to Device Dissemination with 3D Printing

##### 4.6.1. From Cumbrous PDMS Inlets to Intuitive 3D-Printed Modular Architectures that Incorporate Standardized User Interfaces

Although microfluidics is now a mature field,<sup>[1]</sup> in the last 30 years, the soft lithography community has not been able to agree on a simple standard for tubing and inlet/outlet connectors. A device with 16 input fluid lines and 20 control pneumatic lines as shown in Figure 1<sup>[83a]</sup> can be daunting to interface with. Part of the problem is due to the economics of how we do research: We are rewarded for proof-of-concept studies, not for sleek devices; punching inlets into PDMS has worked fine until now. As society and the funding agencies push for research to be translated into products, however, user friendliness has suddenly taken center stage. We believe that 3D printing will rapidly engage the community into adopting connector and inlet modules that represent existing industry standards.

Modular design is an inherent part of 3D printing. With 3D printing, the designer of the microfluidic device has no other choice but to fully specify the packaging (e.g., interface, connectors) in CAD software prior to printing. SL-printed plastic 3D circuits with packaged connectors can be built as interlocking modules and are easy to operate<sup>[117]</sup> (Figure 15 a,b). Importantly, a robust, reliable mixer could be built from assembling various modules,<sup>[117c]</sup> dispelling the popular notion that such modular systems tend to disrupt flow and increase user error and dead volume. It could be argued that post-fabrication assembly of the modules is not an effective strategy because it does not use the full capabilities of SL (which is an assembly-free fabrication technique); indeed, in some instances, assembly of the modules may require metal pins or O rings to prevent leakage.<sup>[117d]</sup> In any case, the concept of “modular design” can be extended beyond physical modules to produce designs by joining various digital modules. An eloquent call for modularity in the design of microfluidic systems was made in the field of droplet engineering.<sup>[118]</sup> Medical-grade (industry-standard) connectors such as Luer Lock or barb-type connectors can be imported from a free repository and copied/pasted into the CAD design before printing<sup>[12]</sup> (Figure 15c), resulting in devices that are more user-friendly than their PDMS or

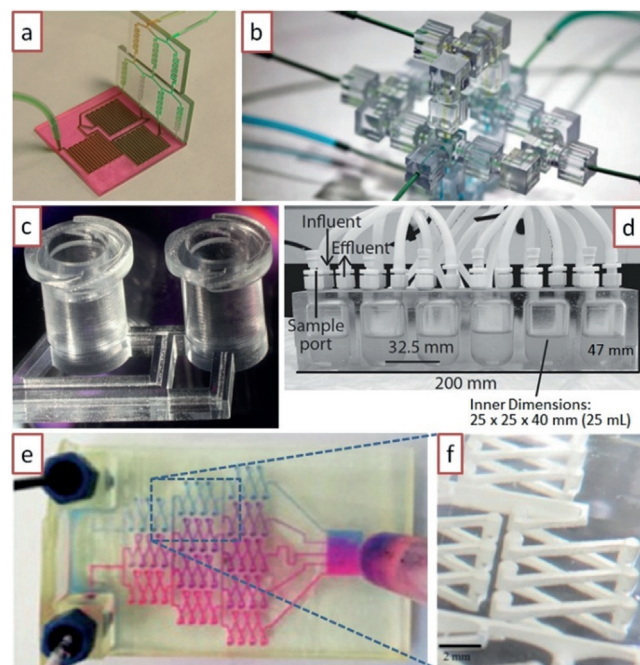


**Figure 15.** Modular microfluidics. a) A modular mixer built by SL. b) A modular droplet generator built by SL. c) An example of user-friendly connectivity (here an industry-standard Luer-Lock connector printed by SL). d) Complex bioreactor printed by SL. e,f) A complex mixer printed with a commercial desktop SL system. Panel (a) reproduced from Ref. [117b] with permission from The Royal Society of Chemistry. Panel (b) reproduced from Ref. [117c]. Copyright 2014 National Academy of Sciences, USA. Panel (c) reproduced from Ref. [12] with permission from The Royal Society of Chemistry. Panel (d) reproduced from Ref. [119] with permission from the American Society for Microbiology. Panels (e) and (f) reproduced from Ref. [120] with permission. Copyright 2014 American Chemical Society.

plastic-molded counterparts. Importantly, digital designs can be inspected and improved by other groups before printing. We predict that teams consisting of mechanical engineers, industrial designers, and interaction/experience designers, will increasingly contribute to microfluidics and improve the functionality of devices. Bioreactors for bacterial cultures<sup>[119]</sup> (Figure 15 d) and microfluidic mixers printed with a desktop printer<sup>[120]</sup> (Figure 15 e,f) are just two examples of future developments. Whereas most PDMS and plastic chips serve as simple “flat containers” for the fluidic architecture of the chip (making sample introduction problematic), with 3D printing, introduction of the sample can be made more intuitive by using boxes or lids that can be opened and closed with hinges, latches, springs, notches, or belts. This new paradigm will facilitate the design of chips made of multiple materials; for example, a saliva or blood sample could be contained on a piece of paper, and the user would only need to deposit it inside a closeable box.

We envision a future dominated by SL printing where microfluidic designs will be available online, and it will be possible to download them and integrate them as modules that will be connected to other devices, modules, or packagings. It seems obvious that SL packagings used by the microfluidics community will soon converge towards user-

friendly interfaces, which will include existing biomedical-standard connectors. Thus we believe that the biggest impact that the 3D printing technology will have in microfluidics will not be the incorporation of “3D piping” but the introduction of modular design paradigms that will amplify the efforts of individual teams.

#### 4.6.2. From PDMS Multi-Layer Valves to 3D-Printable Valves

Fluid handling is a ubiquitous and often tedious operation in biomedicine, ranging from benchtop research that uses cell-culture media to clinical diagnostics with bodily fluids. Most often, fluids are transferred from container to container by means of pipettors that are operated by humans (a tedious and costly mode of operation that is prone to error) or by expensive robotic dispensers. Valves and pumps are essential for automating fluid handling; automation reduces human labor costs, speeds up processing, and enables mass parallelization. The advent of PDMS microvalves and micropumps,<sup>[5a,c]</sup> for example, revolutionized the field of microfluidics and allowed for the miniaturization and automation of a vast array of biomedical assays.<sup>[121]</sup> All-plastic microvalves (to improve the solvent incompatibilities of PDMS) have also been developed.<sup>[104,105,122]</sup> However, the fabrication of valves and pumps is currently expensive because it consists of multiple steps, including molding, machining, bonding, and/or assembling small parts.

Folch and co-workers introduced diaphragm valves and peristaltic pumps that can be 3D-printed by SL<sup>[113]</sup> (Figure 16). A valve in operation is shown in Figure 16b,c. The diaphragm is a 100 µm thick plastic membrane with a diameter of 10 mm that is integrally printed inside a chamber and that can be pneumatically deflected by pressurization of

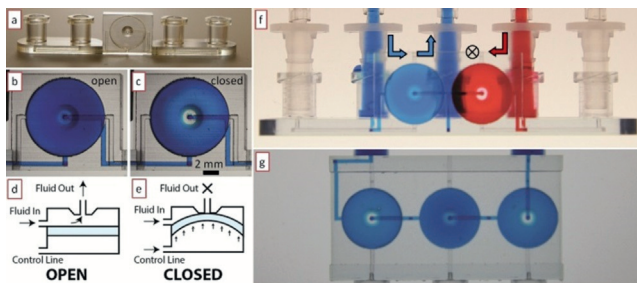


**Figure 16.** 3D-printed valves, switches, and pumps. a) Photograph of a single-valve device 3D-printed in WaterShed XC 11122 resin. b, c) Micrographs showing the dye-filled valve in its open (b) and closed (c) state. d, e) Side view of a valve in its open (d) and closed (e) state. f) Photograph of a switching device set to allow a solution to pass through the valve on the left. g) A peristaltic pump during an actuation phase in which only the middle valve is open. Panels (a)–(g) reproduced from Ref. [87] with permission from The Royal Society of Chemistry.

the control line (Figure 16d,e). 3D-printable valves and pumps can be downloaded as digital objects and incorporated modularly into other devices. Two valves can be used to build a switch (Figure 16f), and three valves can be put together in series to build a peristaltic pump (Figure 16g). No appreci-

able valve leakage was measured in the closed-valve state, even though the membrane is not built of a self-sealing material (e.g., PDMS). The valve closing pressures were reproducible over many valve closing cycles. The fluidic resistance of the valve exhibits a sigmoidal response to control pressure; this multi-state valving behavior could find applications in microfluidic multiplexers,<sup>[123]</sup> flow regulators,<sup>[124]</sup> and fluidic amplifiers.<sup>[125]</sup> 3D-printable valves and pumps can be used to replace costly human labor and robotic pipettors and can be inexpensively printed in transparent biocompatible plastics anywhere in the world. Improvements in the 3D printing process (e.g., resolution, materials) will be required before the valves can be further miniaturized.

#### 4.6.3. From Bulky Control Systems to Autonomous Microfluidics by Using Embedded 3D-Printed Controls

Whereas the above 3D-printed systems are still tethered to bulky control systems requiring computers and electrical signals, work is underway to incorporate 3D-printed automation. Ismagilov and co-workers 3D-printed a “pumping lid” that pressurizes (or pulls vacuum from) the inlet(s) of a microfluidic device<sup>[64]</sup> (Figure 17). The lid consists of two materials and is fabricated by photopolymer inkjet printing; an elastomeric gasket ensures that the lid seals properly to the inlet(s). This simple system altogether eliminates the need for external power in driving microfluidic flow for most applications (the pump lasts for > 2 h).

3D-printed valves could also simplify the fabrication of microfluidic logic elements, such as adding machines,<sup>[10a]</sup> memory latches,<sup>[10b]</sup> shift registers,<sup>[10c]</sup> autonomous pumps,<sup>[10d]</sup> and oscillators.<sup>[10e,f]</sup> We can envision 3D-printed, truly autonomous microfluidic machines with embedded controls (powered by flow or a manually generated pressure differential) that can run pre-programmed biochemical and cell-based assays without the use of pneumatics, electricity, or tubing.

#### 4.6.4. Designs Can Be Disseminated and Sold over the Internet

3D printing minimizes the barriers to manufacturing. Most microfluidic devices are made by PDMS molding or glass etching because these two techniques are inexpensive prototyping techniques that are convenient to the operation and budgets of academic laboratories. Unfortunately, neither PDMS molding nor glass etching allow for large-volume manufacturing, a condition needed for most companies to recover their big initial investments.

Engineers are designers, but thus far they have not had the tools to monetize the products of their research with sufficient agility. MakerBot has created a very vibrant website (“Thingiverse”)<sup>[67]</sup> for sharing CAD designs; however, only designs with non-commercial (Creative Commons) licenses are allowed. Note that in the traditional model of device commercialization, engineers design several prototype iterations until a final prototype is ready for commercial launch. In academia, the various iterations have monetary value to other designers working in a similar field. Based on this simple principle, the company 3DSkema will soon launch an

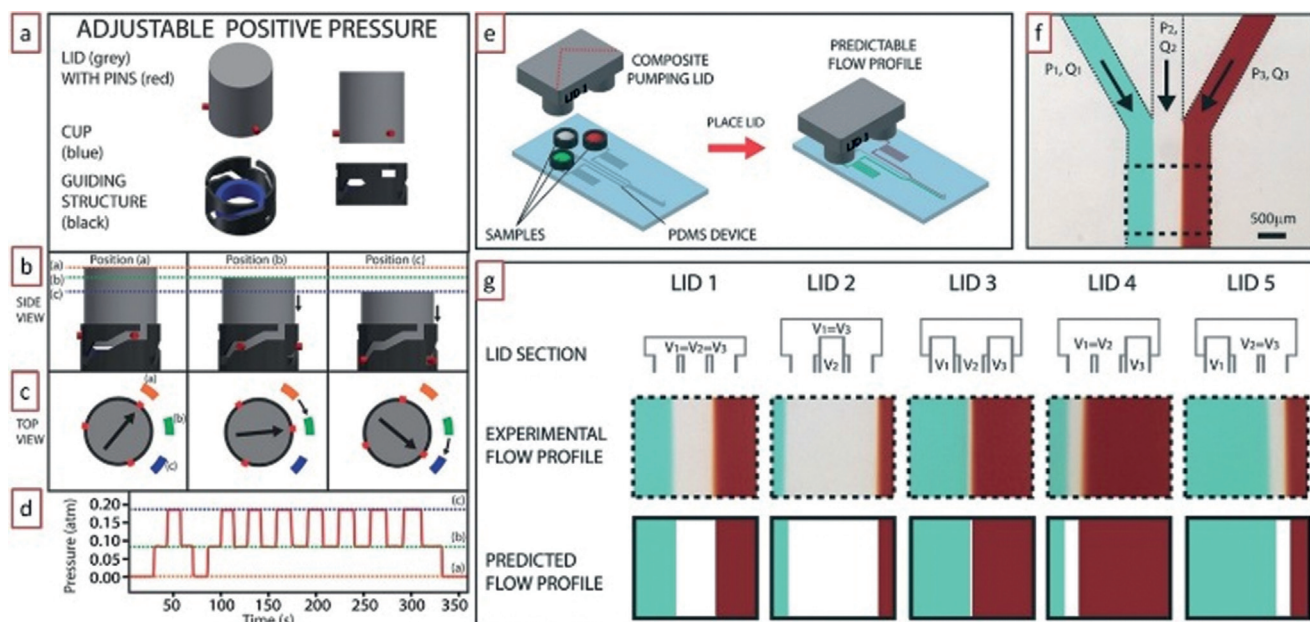


**Figure 17.** 3D-printed “pumping lid”. a) The pumping lid (gray) produces a positive pressure by turning down on a guiding structure that contains a soft elastomeric cup. b, c) The lid can lock at various (a/b/c) positions (indicated by dotted lines or rectangles), each of which produces different pressures. d) Experimental pressure profile obtained by turning the lid between the three positions. A similar design can generate negative pressures. e) A three-cup composite pumping lid for producing three different pressures with the same device. f) Micrograph of the junction at which three channels combine to produce a heterogeneous laminar flow. g) Different composite lids (top row) can be used to produce different flow profiles (middle row) that agree very well with the flow profiles (bottom row) that were predicted based on the pressures produced by the lids and the device geometry. Reproduced from Ref. [64] with permission from The Royal Society of Chemistry.

online marketplace where designers can submit their licensed designs and offer them for sale (or for share with a non-commercial license). This model radically departs from previous commercialization models in that inventors are allowed to monetize their various prototypes without proceeding through the costly patent/plastic product route.

## 5. Summary and Outlook

It has been argued that microfluidics produces very few “killer applications”,<sup>[1,126]</sup> in the sense that it is difficult for microfluidic products to reach the consumer market. Here, we argue that there is no lack of “killer apps”—it is the commercialization pipeline that is obstructed. This obstruction is due to at least three main causes: 1) User interfaces have not reached a standardization point; 2) microfluidic systems still rely on complex control systems; and 3) PDMS-molding processes are not easily commercialized. 3D printing appears to be a suitable technology to address these key points. Still, the application of 3D printing (and in particular SL) to microfluidics is in its infancy. Historically, soft lithography came to dominate the microfluidics field previously occupied by silicon and glass micromachining because PDMS-molded prototypes were cheaper and faster to produce, more biocompatible and transparent, and could incorporate microvalves and micropumps—all despite obvious losses in resolution. However, PDMS microchannels cannot be made with arbitrary aspect ratios, and PDMS flexibility can be a severe problem for the alignment of multiple layers. The

transition from soft lithography to 3D printing is already being marked by a similar set of constraints that can be turned into opportunities:

- 1) Cost versus resolution: DLW/two-photon SL machines, which are prohibitively expensive, and their applications thus have reduced impact, are capable of printing 10 µm wide channels and surface features with approximately 1 µm resolution. Several key SL patents expired in 2014; as a result, there has been a proliferation of new commercial desktop SL printers, and their prices have dropped to an average of less than \$5000. These affordable desktop single-photon SL machines can fabricate features down to 25 µm,<sup>[85]</sup> and smaller (ca. 1 µm) features are expected with newer machines<sup>[37,86]</sup> and lower-viscosity resins. A microfluidic device that is SL-printed by a mail-order service is now already cheaper than a similar device fabricated in PDMS when all factors (materials, salary, time) are taken into account, so the devices that will be printed five years from now should be cheaper and more architecturally complex than the PDMS devices that are being molded today.
- 2) Material development: Most microfluidic engineers are reluctant to use SL (and other 3D printing techniques) because of concerns surrounding the biocompatibility of the resins. However, it should be understood that the use of many SL resins is artificially encouraged for commercial reasons by their developers. Of less interest to commercial developers, some of the most promising resins from a biomedical perspective (e.g., PEG-DA) are inexpensive and patent-free, as they were developed

a long time ago to develop biomaterials (photo-cross-linkable hydrogels) for cell encapsulation. Whereas PDMS does not allow for keeping cells alive or for diffusing large molecules within its matrix, in the next years, as the SL microfluidics community grows, it is to be expected that researchers will produce materials optimized for bio-microfluidic fabrication, including biodegradable and gas-porous matrices. New developments in automated multi-material printing will also have a big impact on sensors and actuators.

- 3) Computer-aided design (CAD): 3D printing device design, unlike soft lithography, is inherently computer-aided and amenable to digital modules. It thus benefits from user-friendly packaging, the use of performance simulation tools, and the electronic dissemination and monetization of the designs. This feature alone is expected to revolutionize the field of microfluidics.
- 4) Fluid automation: We and others have invented 3D-printable elements that are essential for automated fluid handling in microchannels, such as valves and pumps. 3D-printable valves and pumps can be downloaded as digital objects and incorporated modularly into other devices. They can be inexpensively printed in transparent biocompatible plastics from any computer anywhere in the world, and they can be used to replace costly human labor and robotic pipettors.

In summary, additive manufacturing techniques represent a “3D printing revolution” because they are economically extremely efficient: They favor modular and team-based CAD, require neither tooling nor assembly, produce minimal waste, and minimize distribution costs. If (and only if) a large-enough capital investment can be safely invested to run a large-enough production, then a high-throughput fabrication technique such as injection molding is sure to provide the lowest cost per device. Otherwise, for low- to mid-scale production, despite being based on low-throughput serial fabrication, economic considerations usually favor 3D printing techniques against high-throughput molding techniques when all factors are considered. Indeed, the ability to rapidly prototype a physical model in a few hours has already revolutionized the product design process by allowing designers to test designs before investing in tooling or fabrication processes. In biomedicine, shortening the time from prototype to product should enable personalized devices and treatments, accelerate research and development, and help reduce the cost of clinical trials and of the overall access to healthcare.

**How to cite:** *Angew. Chem. Int. Ed.* **2016**, *55*, 3862–3881  
*Angew. Chem.* **2016**, *128*, 3926–3946

- 
- [1] G. M. Whitesides, *Nature* **2006**, *442*, 368.
  - [2] a) P. S. Dittrich, A. Manz, *Nat. Rev. Drug Disc.* **2006**, *5*, 210; b) J. El-Ali, P. K. Sorger, K. F. Jensen, *Nature* **2006**, *442*, 403.
  - [3] E. K. Sackmann, A. L. Fulton, D. J. Beebe, *Nature* **2014**, *507*, 181.
  - [4] Y. N. Xia, G. M. Whitesides, *Angew. Chem. Int. Ed.* **1998**, *37*, 550; *Angew. Chem.* **1998**, *110*, 568.

- [5] a) M. A. Unger, H. P. Chou, T. Thorsen, A. Scherer, S. R. Quake, *Science* **2000**, *288*, 113; b) K. Hosokawa, R. Maeda, *J. Micromech. Microeng.* **2000**, *10*, 415; c) T. Thorsen, S. J. Maerkl, S. R. Quake, *Science* **2002**, *298*, 580.
- [6] A. Folch, *Introduction to BioMEMS*, CRC Press, Boca Raton, FL, **2013**.
- [7] S. K. Sia, G. M. Whitesides, *Electrophoresis* **2003**, *24*, 3563.
- [8] D. Fuard, T. Tzvetkova-Chevolleau, S. Decossas, P. Tracqui, P. Schiavone, *Microelectron. Eng.* **2008**, *85*, 1289.
- [9] a) C. J. Choi, B. T. Cunningham, *Lab Chip* **2007**, *7*, 550; b) T. C. Chang, A. M. Mikheev, W. Huynh, R. J. Monnat, R. C. Rostomily, A. Folch, *Lab Chip* **2014**, *14*, 4540.
- [10] a) E. C. Jensen, W. H. Grover, R. A. Mathies, *J. Microelectromech. Syst.* **2007**, *16*, 1378; b) J. A. Weaver, J. Melin, D. Stark, S. R. Quake, M. A. Horowitz, *Nat. Phys.* **2010**, *6*, 218; c) M. Rhee, M. A. Burns, *Lab Chip* **2009**, *9*, 3131; d) N. S. G. K. Devaraju, M. A. Unger, *Lab Chip* **2012**, *12*, 4809; e) B. Mosadegh, C.-H. Kuo, Y.-C. Tung, Y.-s. Torisawa, T. Bersano-Begey, H. Tavana, S. Takayama, *Nat. Phys.* **2010**, *6*, 433; f) P. N. Duncan, T. V. Nguyen, E. E. Hui, *Proc. Natl. Acad. Sci. USA* **2013**, *110*, 18104.
- [11] C. M. Ho, S. H. Ng, K. H. Li, Y. J. Yoon, *Lab Chip* **2015**, *15*, 3627.
- [12] A. K. Au, W. Lee, A. Folch, *Lab Chip* **2014**, *14*, 1294.
- [13] a) L. Murr, E. Esquivel, S. Quinones, S. Gaytan, M. Lopez, E. Martinez, F. Medina, D. Hernandez, E. Martinez, J. Martinez, S. Stafford, D. Brown, T. Hoppe, W. Meyers, U. Lindhe, R. Wicker, *Mater. Charact.* **2009**, *60*, 96; b) C. A. Terrazas, S. M. Gaytan, E. Rodriguez, D. Espalin, L. E. Murr, F. Medina, R. B. Wicker, *Int. J. Adv. Manuf. Technol.* **2014**, *71*, 33.
- [14] a) A. Mazzoli, *Med. Biol. Eng. Comput.* **2013**, *51*, 245; b) B. Duan, M. Wang, *MRS Bull.* **2011**, *36*, 998.
- [15] D. A. Zopf, S. J. Hollister, M. E. Nelson, R. G. Ohye, G. E. Green, *New Engl. J. Med.* **2013**, *368*, 2043.
- [16] <http://www.renishaw.com/>.
- [17] M. T. Lee, D. Lee, A. Sherry, C. P. Grigoropoulos, *J. Micro-mech. Microeng.* **2011**, *21*, 095018.
- [18] A. Pilipović, P. Raos, M. Šercer, *Int. J. Adv. Manuf. Technol.* **2009**, *40*, 105.
- [19] D. G. Ahn, J. Y. Lee, D. Y. Yang, *J. Mech. Sci. Technol.* **2006**, *20*, 19.
- [20] Y. L. Cheng, S. J. Chen in *Progress on Advanced Manufacture for Micro/Nano Technology 2005, Pt. 1 and 2, Vol. 505–507* (Eds.: W. Jywe, C. L. Chen, K. C. Fan, R. F. Fung, S. G. Hanson, W. H. Hsieh, C. L. Hsu, Y. M. Huang, Y. L. Hwang, G. Jager, Y. R. Jeng, W. Li, Y. S. Liao, C. C. Lin, Z. C. Lin, C. K. Sung, C. H. Tzeng), **2006**, pp. 1063.
- [21] B. O. Erbano, A. C. Opolski, M. Olandoski, J. A. Foggiatto, L. F. Kubrusly, U. A. Dietz, C. Zini, M. M. Makita Arantes Marinho, A. G. Leal, R. Ramina, *Acta Cir. Bras.* **2013**, *28*, 756.
- [22] S. G. Bucella, G. Nava, K. C. Vishunubhatla, M. Caironi, *Org. Electron.* **2013**, *14*, 2249.
- [23] <http://www.stratasys.com/3d-printers/production-series/fortus-900mc>.
- [24] Y. L. Kong, I. A. Tamargo, H. Kim, B. N. Johnson, M. K. Gupta, T.-W. Koh, H.-A. Chin, D. A. Steingart, B. P. Rand, M. C. McAlpine, *Nano Lett.* **2014**, *14*, 7017.
- [25] K. Sun, T.-S. Wei, B. Y. Ahn, J. Y. Seo, S. J. Dillon, J. A. Lewis, *Adv. Mater.* **2013**, *25*, 4539.
- [26] J. T. Muth, D. M. Vogt, R. L. Truby, Y. Mengüç, D. B. Kolesky, R. J. Wood, J. A. Lewis, *Adv. Mater.* **2014**, *26*, 6307.
- [27] J. J. Adams, E. B. Duoss, T. F. Malkowski, M. J. Motala, B. Y. Ahn, R. G. Nuzzo, J. T. Bernhard, J. A. Lewis, *Adv. Mater.* **2011**, *23*, 1335.
- [28] A. Joe Lopes, E. MacDonald, R. B. Wicker, *Rapid Prototyping J.* **2012**, *18*, 129.

- [29] M. S. Manoor, Z. Jiang, T. James, Y. L. Kong, K. A. Malatesta, W. O. Soboyejo, N. Verma, D. H. Gracias, M. C. McAlpine, *Nano Lett.* **2013**, *13*, 2634.
- [30] D. A. Bartholomeusz, R. W. Boutte, J. D. Andrade, *J. Microelectromech. Syst.* **2005**, *14*, 1364.
- [31] a) T. Himmer, T. Nakagawa, M. Anzai, *Comput. Ind.* **1999**, *39*, 27; b) T. Obikawa, M. Yoshino, J. Shinozuka, *J. Mater. Process. Technol.* **1999**, *89–90*, 171.
- [32] C. Hull, *Mod. Cast.* **1988**, *78*, 38.
- [33] a) T. Nakamoto, K. Yamaguchi, P. A. Abraha, K. Mishima, *J. Micromech. Microeng.* **1996**, *6*, 240; b) A. Bertsch, P. Bernhard, C. Vogt, P. Renaud, *Rapid Prototyping J.* **2000**, *6*, 259.
- [34] A. Waldbaur, H. Rapp, K. Lange, B. E. Rapp, *Anal. Methods* **2011**, *3*, 2681.
- [35] A. Bertsch, S. Zissi, J. Y. Jezequel, S. Corbel, J. C. Andre, *Microsyst. Technol.* **1997**, *3*, 42.
- [36] Y. Y. Pan, C. Zhou, Y. Chen, *J. Manuf. Sci. Eng. Trans. ASME* **2012**, *134*, 051011.
- [37] J. R. Tumbleston, D. Shirvanyants, N. Ermoshkin, R. Janusziewicz, A. R. Johnson, D. Kelly, K. Chen, R. Pischmidt, J. P. Rolland, A. Ermoshkin, E. T. Samulski, J. M. DeSimone, *Science* **2015**, *347*, 1349.
- [38] a) <http://www.gizmo3dprinters.com.au/>; b) <http://www.prismlab.com/>.
- [39] W. Jonathan, O. W. Martha, T. Paul, B. Mallory, B. Vaijayantee, M. Nicole, K. Kyobum, P. F. John, S. Ali, X. Yueshuo, F. W. Jean, P. L. Donald, S. Jiayang, I. C. Arnold, D. David, *Biofabrication* **2014**, *6*, 015003.
- [40] S. Kawata, H.-B. Sun, T. Tanaka, K. Takada, *Nature* **2001**, *412*, 697.
- [41] <http://www.nanoscribe.de/en/>.
- [42] S. Tasoglu, U. Demirci, *Trends Biotechnol.* **2013**, *31*, 10.
- [43] J. A. Barrona, B. R. Ringeisen, H. Kimb, B. J. Spargoa, D. B. Chrisey, *Thin Solid Films* **2004**, *453–454*, 383.
- [44] a) N. E. Sanjana, S. B. Fuller, *J. Neurosci. Methods* **2004**, *136*, 151; b) E. A. Roth, T. Xu, M. Das, C. Gregory, J. J. Hickman, T. Boland, *Biomaterials* **2004**, *25*, 3707; c) T. Boland, T. Xu, B. Damon, X. Cui, *Biotechnol. J.* **2006**, *1*, 910; d) V. Mironov, T. Boland, T. Trusk, G. Forgacs, R. R. Markwald, *Trends Biotechnol.* **2003**, *21*, 157.
- [45] B. R. Ringeisen, R. K. Pirlo, P. K. Wu, T. Boland, Y. Huang, W. Sun, Q. Hamid, D. B. Chrisey, *MRS Bull.* **2013**, *38*, 834.
- [46] Y. Lu, G. Mapili, G. Suhali, S. C. Chen, K. Roy, *J. Biomed. Mater. Res. Part A* **2006**, *77*, 396.
- [47] K. C. Hribar, P. Soman, J. Warner, P. Chung, S. C. Chen, *Lab Chip* **2014**, *14*, 268.
- [48] L.-H. Han, S. Suri, C. E. Schmidt, S. Chen, *Biomed. Microdevices* **2010**, *12*, 721.
- [49] a) V. Chan, J. H. Jeong, P. Bajaj, M. Collens, T. Saif, H. Kong, R. Bashir, *Lab Chip* **2012**, *12*, 88; b) V. Chan, P. Zorlutuna, J. H. Jeong, H. Kong, R. Bashir, *Lab Chip* **2010**, *10*, 2062; c) L. H. Han, G. Mapili, S. Chen, K. Roy, *J. Manuf. Sci. Eng. Trans. ASME* **2008**, *130*, 021005.
- [50] a) S. P. Grogan, P. H. Chung, P. Soman, P. Chen, M. K. Lotz, S. Chen, D. D. D'Lima, *Acta Biomater.* **2013**, *9*, 7218; b) P. Soman, P. H. Chung, A. P. Zhang, S. C. Chen, *Biotechnol. Bioeng.* **2013**, *110*, 3038; c) P. Soman, B. T. D. Tobe, J. W. Lee, A. M. Winquist, I. Singec, K. S. Vecchio, E. Y. Snyder, S. Chen, *Biomed. Microdevices* **2012**, *14*, 829.
- [51] S. Suri, L.-H. Han, W. Zhang, A. Singh, S. Chen, C. E. Schmidt, *Biomed. Microdevices* **2011**, *13*, 983.
- [52] P. Zorlutuna, J. H. Jeong, H. Kong, R. Bashir, *Adv. Funct. Mater.* **2011**, *21*, 3642.
- [53] R. D. Kamm, R. Bashir, *Ann. Biomed. Eng.* **2014**, *42*, 445.
- [54] a) A. Ovsianikov, A. Deiwick, S. Van Vlierberghe, P. Dubrule, L. Moller, G. Drager, B. Chichkov, *Biomacromolecules* **2011**, *12*, 851; b) A. Ovsianikov, A. Deiwick, S. Van Vlierberghe, M. Pflaum, M. Wilhelm, P. Dubrule, B. Chichkov, *Materials* **2011**, *4*, 288; c) E. Sascha, H. Eva, B. Kirsten, M. Wolfdietrich, K. Hartmut, E. M. T. Günter, G. Arnold, *Biofabrication* **2011**, *3*, 025003.
- [55] J. L. Connell, E. T. Ritschdorff, M. Whiteley, J. B. Shear, *Proc. Natl. Acad. Sci. USA* **2013**, *110*, 18380.
- [56] A. Bertsch, S. Heimgartner, P. Cousseau, P. Renaud, *Lab Chip* **2001**, *1*, 56.
- [57] T. W. Lim, Y. Son, Y. J. Jeong, D. Y. Yang, H. J. Kong, K. S. Lee, D. P. Kim, *Lab Chip* **2011**, *11*, 100.
- [58] R. Nielson, B. Kaehr, J. B. Shear, *Small* **2009**, *5*, 120.
- [59] B. Kaehr, J. B. Shear, *Lab Chip* **2009**, *9*, 2632.
- [60] C. Zhao, C. Wang, R. Gorkin Iii, S. Beirne, K. Shu, G. G. Wallace, *Electrochem. Commun.* **2014**, *41*, 20.
- [61] <http://www.theengineer.co.uk/awards/the-atkins-project/1006253.article>.
- [62] A. J. Capel, S. Edmondson, S. D. R. Christie, R. D. Goodridge, R. J. Bibb, M. Thurstans, *Lab Chip* **2013**, *13*, 4583.
- [63] J. L. Erkal, A. Selimovic, B. C. Gross, S. Y. Lockwood, E. Walton, S. McNamara, R. S. Martin, D. Spence, *Lab Chip* **2014**, *14*, 2023.
- [64] S. Begolo, D. V. Zhukov, D. A. Selck, L. Li, R. F. Ismagilov, *Lab Chip* **2014**, *14*, 4616.
- [65] A. Causier, G. Carret, C. Boutin, T. Berthelot, P. Berthault, *Lab Chip* **2015**, *15*, 2049.
- [66] “International Society for Optics and Photonics”: H. Wang, S. Masood, P. Iovenitti, E. C. Harvey, *International Symposium on Microelectronics and MEMS*, **2001**, pp. 213.
- [67] <http://www.makerbot.com/>.
- [68] M. D. Symes, P. J. Kitson, J. Yan, C. J. Richmond, G. J. T. Cooper, R. W. Bowman, T. Vilbrandt, L. Cronin, *Nat. Chem.* **2012**, *4*, 349.
- [69] D. Therriault, S. R. White, J. A. Lewis, *Nat. Mater.* **2003**, *2*, 265.
- [70] J. S. Miller, K. R. Stevens, M. T. Yang, B. M. Baker, D.-H. T. Nguyen, D. M. Cohen, E. Toro, A. A. Chen, P. A. Galie, X. Yu, R. Chaturvedi, S. N. Bhatia, C. S. Chen, *Nat. Mater.* **2012**, *11*, 768.
- [71] M. K. Gelber, R. Bhargava, *Lab Chip* **2015**, *15*, 1736.
- [72] P. J. Kitson, M. H. Rosnes, V. Sans, V. Dragone, L. Cronin, *Lab Chip* **2012**, *12*, 3267.
- [73] A. W. Martinez, S. T. Phillips, G. M. Whitesides, *Proc. Natl. Acad. Sci. USA* **2008**, *105*, 19606.
- [74] a) K. Macounová, C. R. Cabrera, M. R. Holl, P. Yager, *Anal. Chem.* **2000**, *72*, 3745; b) K. Macounová, C. R. Cabrera, P. Yager, *Anal. Chem.* **2001**, *73*, 1627.
- [75] A. Hatch, A. E. Kamholz, K. R. Hawkins, M. S. Munson, E. A. Schilling, B. H. Weigl, P. Yager, *Nat. Biotechnol.* **2001**, *19*, 461.
- [76] M. S. Munson, C. R. Cabrera, P. Yager, *Electrophoresis* **2002**, *23*, 2642.
- [77] E. A. Schilling, A. E. Kamholz, P. Yager, *Anal. Chem.* **2002**, *74*, 1798.
- [78] E. Garcia, J. R. Kirkham, A. V. Hatch, K. R. Hawkins, P. Yager, *Lab Chip* **2004**, *4*, 78.
- [79] C. Neils, Z. Tyree, B. Finlayson, A. Folch, *Lab Chip* **2004**, *4*, 342.
- [80] S. Sun, M. H. Yang, Y. Kostov, A. Rasooly, *Lab Chip* **2010**, *10*, 2093.
- [81] I. Cho, K. Lee, W. Choi, Y. A. Song, *Int. J. Mach. Tools Manuf.* **2000**, *40*, 1813.
- [82] J. M. Ruano-López, M. Agirregabiria, G. Olabarria, D. Verdoy, D. D. Bang, M. Q. Bu, A. Wolff, A. Voigt, J. A. Dziuban, R. Walczak, J. Berganzo, *Lab Chip* **2009**, *9*, 1495.
- [83] a) G. A. Cooksey, C. G. Sip, A. Folch, *Lab Chip* **2009**, *9*, 417; b) M. Agirregabiria, F. J. Blanco, J. Berganzo, M. T. Arroyo, A. Fullaondo, K. Mayora, J. M. Ruano-Lopez, *Lab Chip* **2005**, *5*, 545; c) M. Zhang, J. Wu, L. Wang, K. Xiao, W. Wen, *Lab Chip* **2010**, *10*, 1199.

- [84] a) J. W. Choi, E. MacDonald, R. Wicker, *Int. J. Adv. Manuf. Technol.* **2010**, *49*, 543; b) C. Zhou, Y. Chen, Z. Yang, B. Khoshnevis in *Annual Solid Freeform Fabrication Symposium*, Austin, Texas, 2011; c) C. Zhou, Y. Chen, Z. G. Yang, B. Khoshnevis, *Rapid Prototyping J.* **2013**, *19*, 153.
- [85] <http://ilios3d.com/en/>.
- [86] <http://www.oldworldlabs.com/>.
- [87] A. K. Au, N. Bhattacharjee, L. F. Horowitz, T. C. Chang, A. Folch, *Lab Chip* **2015**, *15*, 1934.
- [88] P. R. Miller, S. D. Gittard, T. L. Edwards, D. M. Lopez, X. Y. Xiao, D. R. Wheeler, N. A. Monteiro-Riviere, S. M. Brozik, R. Polsky, R. J. Narayan, *Biomicrofluidics* **2011**, *5*, 013415.
- [89] A. Ovsianikov, B. Chichkov, P. Mente, N. A. Monteiro-Riviere, A. Doraiswamy, R. J. Narayan, *Int. J. Appl. Ceram. Technol.* **2007**, *4*, 22.
- [90] T. Matsuda, M. Mizutani, *J. Biomed. Mater. Res.* **2002**, *62*, 395.
- [91] S. D. Gittard, P. R. Miller, R. D. Boehm, A. Ovsianikov, B. N. Chichkov, J. Heiser, J. Gordon, N. A. Monteiro-Riviere, R. J. Narayan, *Faraday Discuss.* **2011**, *149*, 171.
- [92] A. Doraiswamy, C. Jin, R. J. Narayan, P. Mageswaran, P. Mente, R. Modi, R. Auyeung, D. B. Chrisey, A. Ovsianikov, B. Chichkov, *Acta Biomater.* **2006**, *2*, 267.
- [93] J. Stampfl, S. Baudis, C. Heller, R. Liska, A. Neumeister, R. Kling, A. Ostendorf, M. Spitzbart, *J. Micromech. Microeng.* **2008**, *18*, 125014.
- [94] S. J. Leigh, H. T. J. Gilbert, I. A. Barker, J. M. Becker, S. M. Richardson, J. A. Hoyland, J. A. Covington, A. P. Dove, *Biomacromolecules* **2013**, *14*, 186.
- [95] Y. Du, E. Lo, S. Ali, A. Khademhosseini, *Proc. Natl. Acad. Sci. USA* **2008**, *105*, 9522.
- [96] a) C. G. Williams, A. N. Malik, T. K. Kim, P. N. Manson, J. H. Elisseeff, *Biomaterials* **2005**, *26*, 1211; b) K. T. Nguyen, J. L. West, *Biomaterials* **2002**, *23*, 4307.
- [97] N. E. Fedorovich, M. H. Oudshoorn, D. van Geemen, W. E. Hennink, J. Alblas, W. J. A. Dhert, *Biomaterials* **2009**, *30*, 344.
- [98] B. D. Fairbanks, M. P. Schwartz, C. N. Bowman, K. S. Anseth, *Biomaterials* **2009**, *30*, 6702.
- [99] T. Majima, W. Schnabel, W. Weber, *Macromol. Chem. Phys.* **1991**, *192*, 2307.
- [100] a) D. D. McKinnon, A. M. Kloxin, K. S. Anseth, *Biomater. Sci.* **2013**, *1*, 460; b) L. A. Sawicki, A. M. Kloxin, *Biomater. Sci.* **2014**, *2*, 1612; c) C.-C. Lin, K. S. Anseth, *Proc. Natl. Acad. Sci. USA* **2011**, *108*, 6380.
- [101] P. Kim, H. E. Jeong, A. Khademhosseini, K. Y. Suh, *Lab Chip* **2006**, *6*, 1432.
- [102] C. I. Rogers, J. B. Oxborrow, R. R. Anderson, L.-F. Tsai, G. P. Nordin, A. T. Woolley, *Sens. Actuators B* **2014**, *191*, 438.
- [103] P. N. Nge, C. I. Rogers, A. T. Woolley, *Chem. Rev.* **2013**, *113*, 2550.
- [104] I. R. G. Ogilvie, V. J. Sieben, B. Cortese, M. C. Mowlem, H. Morgan, *Lab Chip* **2011**, *11*, 2455.
- [105] W. H. Grover, M. G. von Muhlen, S. R. Manalis, *Lab Chip* **2008**, *8*, 913.
- [106] a) T. C. Merkel, V. I. Bondar, K. Nagai, B. D. Freeman, I. Pinna, *J. Polym. Sci. Part B* **2000**, *38*, 415; b) K. Hosokawa, K. Sato, N. Ichikawa, M. Maeda, *Lab Chip* **2004**, *4*, 181.
- [107] X. L. Wang, X. B. Cai, Q. Q. Guo, T. Y. Zhang, B. Kobe, J. Yang, *Chem. Commun.* **2013**, *49*, 10064.
- [108] E. Wilhelm, C. Neumann, K. Sachsenheimer, T. Schmitt, K. Lange, B. E. Rapp, *Lab Chip* **2013**, *13*, 2268.
- [109] J. Mai, L. Fok, H. F. Gao, X. Zhang, M. M. Poo, *J. Neurosci.* **2009**, *29*, 7450.
- [110] K. Ohtani, M. Tsuchiya, H. Sugiyama, T. Katakura, M. Hayakawa, T. Kanai, *J. Oleo Sci.* **2014**, *63*, 93.
- [111] T. Kanai, K. Ohtani, M. Fukuyama, T. Katakura, M. Hayakawa, *Polym. J.* **2011**, *43*, 987.
- [112] M. Li, D. P. Kim, *Lab Chip* **2011**, *11*, 1126.
- [113] See Ref. [87].
- [114] X. Zhang, X. N. Jiang, C. Sun, *Sens. Actuators A* **1999**, *77*, 149.
- [115] J. W. Lee, I. H. Lee, D.-W. Cho, *Microelectron. Eng.* **2006**, *83*, 1253.
- [116] P. Amend, O. Hentschel, C. Scheitler, M. Baum, J. Heberle, S. Roth, M. Schmidt, *J. Laser Micro/Nanoeng.* **2013**, *8*, 276.
- [117] a) P. K. Yuen, *Lab Chip* **2008**, *8*, 1374; b) P. K. Yuen, J. T. Bliss, C. C. Thompson, R. C. Peterson, *Lab Chip* **2009**, *9*, 3303; c) K. C. Bhargava, B. Thompson, N. Malmstadt, *Proc. Natl. Acad. Sci. USA* **2014**, *111*, 15013; d) K. G. Lee, K. J. Park, S. Seok, S. Shin, D. H. Kim, J. Y. Park, Y. S. Heo, S. J. Lee, T. J. Lee, *RSC Adv.* **2014**, *4*, 32876.
- [118] B. Kintses, L. D. van Vliet, S. R. A. Devenish, F. Hollfelder, *Curr. Opin. Chem. Biol.* **2010**, *14*, 548.
- [119] C. D. Robinson, J. M. Auchtung, J. Collins, R. Britton, *Infect. Immun.* **2014**, *82*, 2815.
- [120] A. I. Shallan, P. Smejkal, M. Corban, R. M. Guijt, M. C. Breadmore, *Anal. Chem.* **2014**, *86*, 3124.
- [121] a) J. W. Hong, Y. Chen, W. F. Anderson, S. R. Quake, *J. Phys. Condens. Matter* **2006**, *18*, S691; b) J. Melin, S. R. Quake, *Annu. Rev. Biophys. Biomol. Struct.* **2007**, *36*, 213.
- [122] P. Gu, T. Nishida, Z. H. Fan, *Electrophoresis* **2014**, *35*, 289.
- [123] D. W. Lee, Y.-H. Cho, *Lab Chip* **2009**, *9*, 1681.
- [124] E. W. Lam, G. A. Cooksey, B. A. Finlayson, A. Folch, *Appl. Phys. Lett.* **2006**, *89*, 164105.
- [125] R. Furlan, J. N. Zemel, *Sens. Actuators A* **1995**, *51*, 239.
- [126] a) P. Gould, *Mater. Today* **2004**, *7*, 48; b) A. P. Lee, *Highlights Chem. Technol.* **2009**, *5*.

Received: May 14, 2015

Published online: February 8, 2016